

國立交通大學
光電工程研究所

碩士論文

利用微米透鏡陣列與表面粗化加強垂直式
氮化鎵發光二極體發光強度



**Light output enhancement of GaN vertical
light emitting diode using micro-lens array
and surface roughening**

研究生：葉剛帆

指導教授：王興宗教授

郭浩中教授

中華民國九十五年六月

利用微米透鏡陣列與表面粗化加強垂直式氮化鎵發光二極
體發光強度

Light output enhancement of GaN vertical light emitting diode
using micro-lens array and surface roughening

研究生:葉剛帆

Student : Kang-fan Yeh

指導教授:王興宗 教授

Advisor : Shing-Chung Wang

郭浩中 教授

Hao-chung Kuo



A Thesis

Submitted to Institute of Electro-Optical Engineering
College of Electrical Engineering and Computer Science

National Chiao Tung University

in Partial Fulfillment of the Requirements

for the Degree of

Master

In

Electro-Optical Engineering

June 2006

Hsinchu, Taiwan, Republic of China

利用微米透鏡陣列與表面粗化加強垂直式氮化鎵發光二極體發光強度

研究生:葉剛帆

指導教授:王興宗 教授

郭浩中 教授

交通大學光電工程研究所

摘要

在本篇論文中，主要是探討垂直式氮化鎵發光二極體在表面製作微米透鏡陣列與表面粗化的製成技術與特性量測。在第一部分，我們利用雷射剝離技術成功的製做出垂直式氮化鎵發光二極體，並且在利用光阻溢流與乾式蝕刻將微米透鏡陣列製作在元件的表面，微米透鏡的尺寸為 3、5、10、15、20 微米，在量測的結果部分，在發光波長在 460 奈米下，垂直面的光增強了 30%~15%相較於沒有製作微米透陣列的垂直式氮化鎵發光二極體。

另一部份，則是在垂直式氮化鎵發光二極體的表面製造粗化的效果，以來增進光從發光二極體中萃取出效率，利用乾式蝕刻將表面製造出粗化的效果，再利用標準的黃光微影製成技術，因此成功的製造出 n 型表面粗化的垂直式氮化鎵發光二極體，至於出光強度的增強量會隨者表面粗化情況的不同有著 30%~110% 的增強相較於沒有在表面製造粗化的垂直式氮化鎵光光二極體。

Light output enhancement of GaN vertical light emitting diode using micro-lens array and surface roughening

Student: Kang-fan Yeh

Advisors: Dr. Shing-chung Wang

Dr. Hao-chung Kuo

Institute of Electro-Optical Engineering
National Chiao Tung University

Abstract

In the thesis, we report the GaN vertical light emitting diodes with micro lens array and surface roughening. The first part, GaN-based vertical light-emitting diodes (VLEDs) were fabricated by a laser lift-off (LLO) process and the effects of micro lens formation by plasma etching on GaN-based VLED devices were investigated. By forming a 3, 5, 10, 15 and 20um micro lens array on the GaN-based VLEDs, the measured light emission intensities at 460nm and in the direction normal to the surface of the device increased 30%~15% compared with those of the GaN-based VLED without the micro lens array.

In second part, roughened surfaces of light emitting diodes provide substantial improvement in light extraction efficiency. By using the laser-lift-off technique followed by plasma etching process to roughen the surface, the VLEDs with n-GaN surface roughening has been fabricated. The enhancement of the VLED output power depends on the surface conditions. The output power of an optimally roughened surface VLED shows 30% to 110% increase compared to that of a conventional VLED.

誌謝

鳳凰花開時，驪歌響起，這個屬於畢業的夏季也隨者這篇論文的收尾展開了！回首在學校的兩年，一切彷彿都已經成為我腦海中的寶貴回憶，踏遍 NDL 的個個角落，兩年來的記憶，一股腦的全衝上了心頭，各式各樣的機台編織了這篇論文的撰寫，實驗的過程深深的被烙印，點點滴滴都令我無法忘懷。陪伴著我走過這段黃光室歲月的人們，我抱著無限的感激：小強、小朱學長細心的指導，宗頂是最好的戰友，柏傑與黃仲為這裡帶來歡笑，因為有你們讓這冷冰冰的製成室裡好不寂寞！越過了荷花池來到了 401，文凱那日漸肥胖的身軀述說著大夥出遊那份玩耍的快樂，意偵與游敏在實驗上的協助，歷歷在目，心中的感謝無法用簡單的言語形容。雙手輕放在光學儀器上，慢慢的閉上眼，這裡我擁有過的實驗失落、疑惑、喜悅與成功的記憶，瞬間在腦中再一次的上演著。

最後回到了 250，一個屬於我最熟悉的地方，歡笑、垃圾話與老闆們的攻防戰，每天都不斷在這重複，志堯、學弟妹、麗君助理，都是這裡不可或缺的角色，因為有大夥，讓這塊屬於 250 的畫版，彩繪出令人無法忘懷的顏色。老闆，這個在碩士班屬於老師的代名詞，我深刻的體驗到了，兩年來的教導讓我獲益良多，王興宗老師的指導、郭浩中老師的託付、盧廷昌老師的糾正，雖然只是簡簡單單的行為，但帶給我的卻是日後受用不盡的寶貴經驗。驪歌似乎已經演奏到最後一小段了，要感謝的人，似乎來不及述說，但願那份發自我內心深處最由衷的感謝能傳到每一個幫助過我的人。最後我將此論文獻給支持我的親人，希望我沒讓他們失望。或許是到了說再見的時刻，心中的不捨與依戀是該放下了，這刻起我會以半導體雷射技術實驗室為榮，當方帽向天空拋去的那一刻起，象徵大夥各奔東西之時，願在不久的將來，還有再聚首的一天。

剛帆 2006 7/4 於交通大學

Content

Abstract (in Chinese).....	i
Abstract (in English).....	ii
Acknowledgement.....	iii
Content.....	iv
List of Figures.....	vi
List of Tables.....	viii
Chapter 1 Introduction.....	1
Chapter 2 The discussion of vertical light emitting diode structure.....	5
2-1 Basic Structure of GaN LED.....	5
2-1.1 Sapphire Substrate.....	6
2-1.2 Emitting Area of GaN LEDs.....	8
2-2 Laser Lift-off Process of GaN Thin Film.....	9
2-2.1 Sample Preparation.....	10
2-2.2 Freestanding GaN Thin Film Fabrication.....	10
2-3 The structure of vertical light emitting diodes	11
2-3.1 GaN LED Structure.....	11
2-3.2 The processing of VLEDs.....	11
Chapter 3 The progress of dry etching using by ICP-RIE.....	16
3-1 Micro-lens formed by re-flow of photoresist.....	16
3-2 The etching result of micro lens array by ICP-RIE.....	17
3-3 The progress of surface roughening for VLEDs.....	21
Chapter4 Fabrication and Characteristics of Micro-lens Array LEDs.....	26
4-1 Fabrication of GaN-Based Micro-lens Array LEDs.....	26
4-2 Characteristics of GaN-Based Micro-lens Array LEDs.....	27
4-3 Simulation of GaN VLEDs with micro lens array.....	28

4-3.1 Simulation software – TracePro.....	29
4-3.2 Simulation of VLEDs with Micro Lens Array by Tracepro.....	30
Chapter5 Fabrication and Characteristics of Roughening LEDs.....	40
5-1 Fabrication of GaN-Based roughening LEDs.....	40
5-2 Characteristics of GaN-Based roughening LEDs.....	41
Chapter6 Conclusion.....	46



List of Figures

Figure2-1	The basic structure of GaN.....	14
Figure2-2	The process scheme for fabrication of LLO un-doped GaN.....	14
Figure2-3	The processing of vertical light emitting diodes.....	15
Figure3-1	The progress of micro lens formed by re-flow of photoresist.....	17
Figure3-2	The SEM images of etching result, the micro lens is fabricated on the basic structure.....	18
Figure3-3	The SEM images of etching result, the micro lens is fabricated on vertical light emitting diode.....	18
Figure3-4	With increasing the ratio of BCl ₃ , the SEM image of etching result.....	19
Figure3-5	As the bias decreasing, the SEM images of etching result.....	20
Figure3-6	The final result for micro lens array on vertical light emitting diodes....	20
Figure3-7	The AFM image of micro-lens.....	21
Figure3-8	AFM image of an N-face GaN surface etched by ICP-RIE(a)conventional devices (b)1-min etching (c) 3.5-min etching and (d) 5-min etching.....	23
Figure3-9	(a) shows the image of SEM for etching time=3.5min. (b) The image of SEM that compared surface before etching and after etching	25
Figure3-10	The TEM image of roughening surface.....	25
Figure4-1	The processing of the GaN vertical light emitting diodes with micro-lens array.....	33
Figure4-2	The SEM image of the GaN micro-lens array.....	33
Figure4-3	The probe-station system is used for electronically characteristic.....	34
Figure4-4	Curves of current-voltage (I-V) of VLEDs with micro lens array and a conventional VLED fabricated from the same wafer.....	34
Figure4-5	Light output power of VLEDs with micro lens array and a conventional LED as functions of injected current density. The insert shows the	

	enhancement-lens size curves.....	35
Figure4-6	The VLEDs with 3um lens array have injected 0.5 mA and 1.0 mA	35
Figure4-7	The same coverage for the different size lens. Light output power of VLEDs with micro lens array and a conventional LED as functions of injected current density. The insert shows the enhancement-lens size curves.....	36
Figure4-8	An irradiance map of GaN VLEDs with micro lens array of 300×300 μm ² simulated from the Trace Pro program.....	36
Figure4-9	Light intensity distributed from the surface of detector box that is most next to the top surface of device by Trace Pro.....	37
Figure4-10	(a) the experiment that fixed the space with different size of micro lens compared with simulation results. (b) the experiment that same coverage of micro lens compared with simulation results.....	37
Figure4-11	The light cone for photon escaping outsider is the largest as the curvature center of micro –lens is located at MQW.....	38
Figure5-1	The processing of the GaN vertical light emitting diodes with surface roughening	43
Figure5-2	Plan-view microphotographs of a VLED bonded on a Si substrate: (a) conventional surface (b) after roughening the surface.....	44
Figure5-3	Curves of current-voltage (I-V) of VLEDs with surface roughening and a conventional VLED fabricated from the same wafer.....	44
Figure5-4	Light output power of VLEDs with surface roughening and a conventional LED as functions of injected current density.....	45
Figure5-5	The VLEDs with surface roughening and conventional VLEDs at the same injected current 1mA.....	45

List of Tables

Table 4-1	The height of different size of micro lens.....	39
Table 4-2	Parameters for the light-tracing simulation of VLED with micro lens array.....	39



Chapter 1

Introduction

The group III-nitride wide band gap semiconductors have recently attracted considerable interest due to their potential applications in optoelectronics devices, such as light emitting diodes (LEDs) and laser diodes (LDs) , The gallium nitride (GaN)-based light emitting diodes have been intensively studied for use in full-color outdoor LED displays, LED lighting and so on. [1.1-6] In particular, researchers are currently making efforts to develop highly bright LEDs for white LEDs,

Despite the advancement in GaN , the primary impediment to the GaN is its thermal decomposition at relatively low temperature to produce metallic Ga and N₂ gas.[1.7-8] As a result, large area GaN substrates are still difficult to fabricate, necessitating heteroepitaxial growth of GaN thin film on to dissimilar substrates such as sapphire or SiC.[1.9-10] The GaN crystal structure , combine with the high GaN growth temperatures make deposition of high quality material directly onto common semiconductor substrate such as Si or GaAs very difficult.

The sapphire is the most commonly used substrate because of it is relatively low cost. However, due to the lattice and thermal expansion coefficient mismatch between the sapphire and GaN.[1.11] The disparate properties of these two materials results in high density of extended defect, such as dislocations and stacking fault, at the GaN/substrate interface.[1.12]

Due to the poor electrical and thermal conductivity of sapphire substrate, many group have attempted to integrate GaN with other more conductive materials. A more conductive substrate could allow backside ohmic contacts to GaN-based devices unattainable with sapphire substrate. For GaN-based devices processed on sapphire, all contacts of p- and n- electrode must be made from the topside. The device process

steps are relatively complicated compared with other compound semiconductor devices. The poor thermal conductivity of sapphire also prevent efficient dissipation of heat generated by high current devices, such as LDs and high power transistors, consequently limiting device performance.[1.13]

Therefore, freestanding GaN optoelectronic devices without sapphire substrate are most desirable. The transformation of GaN with other substrates could take advantages of the favorable function of different material systems. For fabrication freestanding GaN light emitting diodes several techniques may be used to achieve including material deposition, bonding of different elements, lift-off, and layer transfer. In these techniques, the combination of wafer bonding and device layer lift-off present the major part to join the GaN device layer with dissimilar materials.

Recently, the laser lift-off (LLO) technique has been used to fabricate the freestanding GaN LEDs. [1.14-15] The LLO process should be also applicable to other GaN-based optoelectronics devices and in particular suitable for high light output power, high operation current, high heat dissipation capacity, and large area emission. For GaN based LEDs, the external quantum efficiency of the nitride-based LEDs is often low due to the large refractive index difference between the nitride epitaxial layer and air. $[\theta_c = \sin^{-1}(n_{air} / n_{GaN})] \sim 23^\circ$

In this study, the reversely constructed GaN-based vertical LEDs (VLEDs), with n-GaN on top were fabricated by laser lift-off process. The methodology for the freestanding GaN-based light emitting diodes transferred to electrical and thermal conductivity Si substrate is demonstrated. As two ways of texturing the n-GaN located on top of the device, micro-lens arrays and surface roughening were formed by a plasma etch process and its effect on the light extraction efficiency and the angular distribution of the emitted light were investigated and compared with those by a

planar surface LLO GaN-based VLEDs

This thesis is organized in the following manner. In chapter 2 we will talk about the vertical light emitting diodes structure and compare the conventional LEDs on sapphire. In chapter 3 we will introduce the dry etching process performed by using inductively coupled plasma (ICP). In chapter 4, the content is mainly divided into two parts. The first is fabrication of GaN-based micro-lens array LEDs. Second is Characteristics of GaN-based micro-lens array LEDs. The chapter 5 is the fabrication and characteristics of the surface roughening LEDs. Finally, our conclusions are mentioned in the chapter 6.



Reference

- [1.1]R. K. Chang and A. J. Campillo, Optical Processes in Microcavities, World Scientific, Singapore (1996).
- [1.2]R. A. Mair, K. C. Zeng, J. Y. Lin, H. X. Jiang, B. Zhang, L. Dai, A. Botchkarev, W. Kim, H. Morkoc, and M. A. Khan, Appl. Phys. Lett. 72, 1530 (1998).
- [1.3]K. C. Zeng, L. Dai, J. Y. Lin, and H. X. Jiang, Appl. Phys. Lett. 75, 2563 (1999).
- [1.4]R. A. Mair, K. C. Zeng, J. Y. Lin, H. X. Jiang, B. Zhang, L. Dai, H. Tang, A. Botchkarev, W. Kim, and H. Morkoc, Appl. Phys. Lett. 71, 2898 (1997).
- [1.5]R. A. Mair, K. C. Zeng, J. Y. Lin, H. X. Jiang, B. Zhang, L. Dai, A. Botchkarev, W. Kim, H. Morkoc, and M. A. Khan, Appl. Phys. Lett. 72, 1530 (1998).
- [1.6]H. X. Jiang, J. Y. Lin, K. C. Zeng, and W. Yang, Appl. Phys. Lett. 75, 763 (1999)
- [1.7]Z.A. Munir, and A.W. Searcy, J. Chem. Phys. 42, 4233(1965)
- [1.8]N. Newman, J. Ross, and M. Rubin, Appl. Phys. Lett. 62, 1242(1993)
- [1.9]S. Nakamura, M. Senoh, and T. Mukai, Appl. Phys. Lett. 62, 2390(1993)
- [1.10]H. Amano, M. Kito, K. Hiramatsu, and I. Akasaki, Jpn. J. Appl. Phys. 28, L21(1989)
- [1.11]S.D. Lester, F.A. Ponce, M.G. Craford, and D.A. Steigerwald, Appl. Phys. Lett. 66, 1249(1996)
- [1.12]I. Akasaki, H. Amano, Y. Koiddde, K. Hiramatsu, and N Sawaki, J. Cryst. Growth 98, 209 (1989)
- [1.13]A.T. Ping, Q. Chen, J.W. Yang, M.A. Khan, I. Adesidda, IEEE Electron Device Letters 19, 54 (1998)
- [1.14]W. S. Wong, T. Sands, N. W. Cheung, M. Kneissl, D. P. Bour, P. Mei, L. T. Romano, and N. M. Johnson, Appl. Phys. Lett. 75, 1360 (1999)
- [1.15] W. S. Wong, T. Sands, N. W. Cheung, M. Kneissl, D. P. Bour, P. Mei, L. T. Romano, and N. M. Johnson, Appl. Phys. Lett. 77,2822 (2000)

Chapter 2

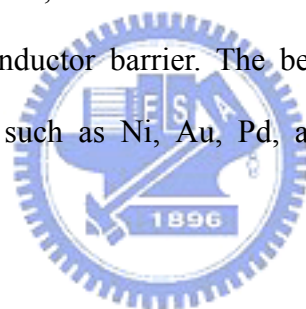
The discussion of vertical light emitting diode structure

2-1 Basic Structure of GaN LED

The brightest devices use either a single or multiple quantum well structure. (Figure2-1) A typical complete device structure consists of a low-temperature deposited GaN or AlN buffer layer on c-plane sapphire, a 3-4 μ m silicon-doped GaN layer, a SQW or multiple quantum well (MQW), a 1000Å magnesium-doped AlGaIn layer, and a 3000Å magnesium-doped GaN layer. The commercial high-brightness candela-class blue LED devices employed an intentional Zn-Si impurity complex in the InGaIn active region to produce blue LEDs with a broad emission spectrum centered at 450nm. The output power was as high as 1.5mW, corresponding to an external quantum efficiency of 2.7% and a luminous efficiency of 2.1 lumens/watt. External quantum efficiency refers to the ratio of the number of photons produced to the electrical current crossing the PN-junction, in units of photons/electron. Luminous efficiency refers to the extent of the human-eye response per unit of input power to the LED. The human-eye response is greatest in the green spectral region and drops as the wavelength goes to the ultraviolet or infrared region.

The variety of high-brightness blue[2.1] and green[2.2] LEDs were reported during 1995. This second generation of commercial III-V nitride LED products, based on a SQW structure, dramatically improved the efficiency and the color purity for blue-green and green LEDs. Reported output power values for 450nm blue and 525 nm green LEDs are 4.8mW, and 3.0mW, respectively, corresponding to luminous-efficiency values of approximately 3.0 lumens/watt and 22.0 lumens/watt, respectively. Nichia Chemical Company of Japan has commercialized LEDs with this SQW structure and produces devices with wavelengths of 470nm blue, 495nm

blue-green, and 525nm green with efficiencies that significantly exceed these reported values. The spectral width of these commercial LEDs and, hence, results in a greatly improved color purity or saturation. However, the shift of color with increasing operating current remains a concern for this technology. The blue (AlIn)GaN LEDs commercially have a typical forward voltage of 3.5-3.6V when driven by a current of 20mA. One would expect the forward voltage to correspond closely to the energy bandgap in the quantum well, about 2.8-3.0V. Lower forward voltage characteristics are essential for improving laser output and lifetime. One key is improved ohmic contact to the p-type GaN. It is also necessary to carefully choose the metals involved because of the high ionic content of the (AlIn)GaN bonds. Unlike what happens in covalent materials such as silicon, the work function of the metal deposited on p-GaN influences the metal- semiconductor barrier. The best p-contact candidates are the high work -function metals, such as Ni, Au, Pd, and Pt, because they yield low Schottky barrier heights [2.3].



2-1.1 Sapphire Substrate

The semiconductors GaN, AlN, and InN have been grown primarily on sapphire, most commonly the (0001) orientation, but also on the a- and r- planes [2.4]. In addition, the group-III-V nitrides have been grown on SiC, Si, GaAs. With the exception of SiC, the interest in using these substrates has slowly decreased. The primary reason for the decline in interest in the zincblende substrates is the inherent difficulty in growing high quality GaN in the cubic phase. In addition, the high growth temperature involved usually precludes the use of materials with low decomposition temperatures such as GaAs. Due to the reactivity of nitrogen with Si, amorphous Si₃N₄ layers typically form before the GaN deposition, preventing high-quality GaN films on Si [2.5-6] substrates. Currently, the SiC materials system is

challenging the GaN/sapphire system for dominance in both the optoelectronic and electronic arena [2.7]. SiC offers a higher electrical and thermal conductivity compared to sapphire and is available in the hexagonal crystal structure. Despite these advantages, SiC suffers from being substantially more expensive compared to sapphire. The large cost of using SiC has limited its usefulness and availability to only a small number of groups.

The preference for sapphire substrates can be ascribed to its wide availability, hexagonal symmetry, low cost, 2-inch-diameter crystals of good quality, transparent nature, and its ease of handling and pre-growth cleaning. Sapphire is also suitable at high temperatures ($\sim 1000^{\circ}\text{C}$) required for epitaxial growth using the various CVD techniques commonly employed for GaN growth.

However, due to the poor electrical (Electrical resistivity= 10^{11} - 10^{16} ohm-cm) and thermal conductivity (35 W/m-K) of sapphire substrate, the device process steps are relatively complicated compared with other compound semiconductor devices. For devices processed on sapphire substrates, all contacts must be made from the top side. This configuration complicates contact and packaging schemes, resulting in a spreading-resistance penalty and increased operating voltages [2.8]. The heat dissipation of sapphire substrate was poor, therefore the commercial available GaN blue LEDs was typically operated under low current operation conditions.

Therefore, GaN optoelectronics devices fabricated on electrically and thermally conducting substrate by separating sapphire substrate are most desirable. The separation of hydride vapor phase epitaxy (HVPE) grown 2-inch GaN wafer from the sapphire substrate was first demonstrated [2.9] by using the laser lift off (LLO) technique. The pulsed, high power UV laser of third harmonic of Q-switched Nd:YAG laser with 355 nm wavelength was used to irradiate through the transparent sapphire substrate to lift off the GaN film. The physical process responsible for the

lift-off was considered by rapid thermal decomposition of GaN near the sapphire interface. For the LED grown on GaN substrate, the performance of high light output power and high current continuous wave operation condition was reported [2.10]. However, the GaN substrate fabricated by combining HVPE growth and LLO process was substantially more expensive compared to sapphire.

2-1.2 Emitting Area of GaN LEDs

The emission area of conventional GaN-based LEDs on sapphire with the p-side up configuration was limited because the p-GaN and MQW layers required etching away to expose the n-GaN layer for n-type contact and wire bond purpose. In Figures 2-2, the electrical contacts to the p- and n-layers are both on the top surface of the device because of the insulating sapphire substrate. An important consequence for LEDs on sapphire is that since most of the light generated at the junction escapes the device through the top surface, the large-area p-contact [2.11] has to be made as transparent as possible outside the area where electrical bond wires are attached. Typically the p-contact pad with square or circular size of 80-100 μm was fabricated. The p-type ohmic contact of conventional LED devices with semi transparency is required to spread current from the p-bonding pad across the junction area because of the very low conductivity of GaN:Mg [2.12]. This is typically done by deposited a semitransparent ohmic contact metallization across the GaN:Mg surface. Although the technology has matured, there still exist challenges in optimizing the growth of high p-type doping and in device fabrication aspects.

Recently, S. R. Jeon et al. [2.13] demonstrated a buried tunnel contact junctions on the p-side with n-side up configuration to eliminate lateral hole excitation currents . A reverse biased tunnel junction (TJ) supplies holes to the p-type crystal above the active region by lateral electron currents. Furthermore, this concept allows the use of

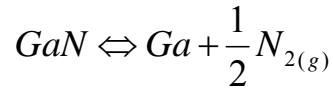
a low-resistivity n-type GaN instead of a high-resistivity p-type GaN as a top contact layer. Thus, the n-type ohmic contact can be used instead of the p-type ohmic contact of conventional LED devices. S. R. Jeon concluded that the tunnel junction allows the use of n-type GaN instead of p-type GaN as a top contact layer in GaN-based devices. The top-emitting light output power of the TJ LED with a lateral current spreading is two times higher than that of the conventional LED with semitransparent metal onto p-type layer. The TJ LEDs also induce a spatially uniform luminescence. Although the turn voltage of these TJ LEDs was still higher than that of the conventional LEDs, the configuration of n-side up GaN LEDs could be a very good idea to obtain a large-area-emission GaN LEDs due to its good current effect of n-type GaN layer.

For other techniques of increasing the emitting area, an interdigitated mesa geometry was recently reported [2.13]. However, the emitting area was still limited due to the current spreading length of p-GaN layer [2.14]. The current spreading length was critical depended on the ratio of semitransparent contact resistance and its thickness [2.15]. In addition, the interdigitated finger circuit patterns on the top of p-GaN also confine the active light of emission area. More recently, the flip chip bonding technique for backside emission of GaN LEDs was reported [2.16]. A large emitting size of about 1 mm× 1mm and high extrication output power from the backside polished sapphire substrate was achieved by flip chip bonding techniques. However, the processes steps of these techniques were relatively complicated.

2-2 Laser Lift-off Process of GaN Thin Film

In this section, the experiment of laser etching GaN thin film will be investigated to establish the laser lift-off condition of GaN. A KrF excimer laser (Lambda Physik LPX210) at wavelength of $\lambda=248$ nm with pulse width of 25 ns was used for LLO technique. The laser irradiation causes the decomposition of GaN into

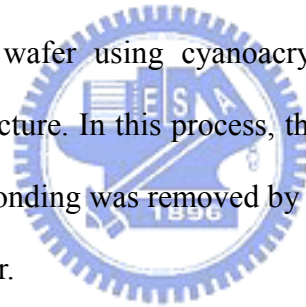
gaseous nitrogen and gallium droplets, following the equation:



The GaN sample after laser irradiation tends to show some material residues such as Ga, and Ga oxide. These residues were then clean up by dilute acid solution such as HCl or H₂SO₄/H₂O₂

2-2.1 Sample Preparation

The LLO process was first conducted using an un-doped GaN sample grown on sapphire substrate. The backside of sapphire was first polished by various size of diamond paste from 3 μm to 1 μm then cut to a sample size of 1 cm×1 cm. The sample was boned to a Si wafer using cyanoacrylate ester adhesive forming a sapphire/u-GaN/epoxy/Si structure. In this process, the residue of epoxy remained on the edge of the sample after bonding was removed by acetone. The sample was placed on the top of workstation in air.



2-2.2 Fabrication of freestanding GaN Thin Film

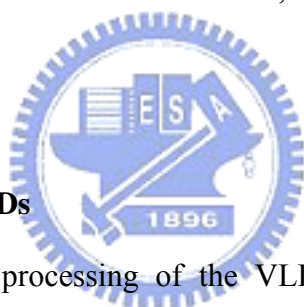
Figure 2-2 shows the LLO process sequence for fabrication of freestanding un-doped GaN film. The pulsed KrF excimer laser was directed through the backside of the polished transparent sapphire substrate and indicated the decomposition of Ga interfacial layer between the GaN and sapphire. By heating the irradiated samples at Ga melting point of 30°C, the GaN film was then easily separated from sapphire substrate and transferred onto the Si supported carrier and the metallic Ga residues was removed to complete the LLO process.

2-3 The structure of vertical light emitting diodes

In this thesis, we used the same structure of vertical light emitting diodes(VLEDs) to do different process procedures such as micro-lens arrays, surface roughening. In this section, we will talk about the structure of our VLEDs.

2-3.1 GaN LED Structure

The GaN-based LED structures were grown by metal organic chemical vapor deposition (MOCVD) on sapphire substrate. The LED wafer has a structure consists of about 25-30nm-thick GaN low –temperature buffer layer, a 2.0-um-thick un-doped GaN layer, 3.5-um-thick highly conductive n-type GaN layer, a MQW region consisting of five periods 2/8-nm-thick InGaN/GaN, and a 0.25-um-thick p-type GaN layer.



2-3.2 The processing of VLEDs

Figure 2.3 show the processing of the VLEDs. At first, the sample was deposited a 5000Å Si_3N_4 thin film layer on GaN-based LED film, followed by photolithography patterning to define the isolation layer of device, then, the sputter evaporated ITO (300 nm) as the transparent contact layer, and fabricated reflective mirror which we evaporated Al (30nm) with electron-beam gun. About bonding metal was In/Au (30/150nm), and Si substrate was evaporated Cr/Au(30/1000nm). Finally, we bond sample and Si substrate at 350°C and used laser lift-off technique to separate original sapphire substrate as shown in Figure 2.3. Then, the structure of VLEDs was finished

Reference

- [2.1] S. Nakamura, M. Senoh, N. Iwasa, and S. Nagahama, *Appl. Phys. Lett.*, 67 1868 (1995).
- [2.2] S. Nakamura, M. Senoh, N. Iwasa, S. Nagahama, T. Yamada, T. Mukai, *Jpn. J. Appl. Phys.*, 34 L1332 (1995).34 L1332 (1995).
- [2.3] T. Mori, T. Kozawa, T. Ohwaki, Y. Taga, S. Nagai, S. Yamasaki, S. Asami, N. Shibata, and M. Koike, *Appl. Phys. Lett.*, 69 3537 (1996).
- [2.4] S. Strite, H. Morkoc, *J. Vac. Sci. Technol. B*10, 1237 (1992).
- [2.5] S.A. Nikishin, N.N. Faleev, V.G. Antipov, S. Francoeur, L. Grave de Peralta, G.A. Seryogin, H. Temkin, T.I. Prokofyeva, M. Holtz, and S.N.G. Chu, *Appl. Phys. Lett.* 75, 2073 (1999).
- [2.6] Chuong A. Tran, A. Osinski, R.F. Karliceck, Jr., I Berishev, *Appl. Phys. Lett.* 75, 1494 (1999).
- [2.7] S. Sriram, G. Augustine, A. Burk, R. Glass, H. Hobogood, P. Orphanos, L. Rowland, T. Smith, C. Brandt, M. Driver, and R. Hopkins, *IEEE Electron. Device Lett.* 17, 369 (1996).
- [2.8] D. L. Barton, M. Osinski, C. J. Helms, N. H. Berg, and B. S. Phillips, *SPIE Int. Soc. Opt. Eng.* 64 2694, (1996).
- [2.9] M. K. Kelly, O. Ambacher, B. Dahlheimer, G. Groos, R. Dimitrov, H. Angerer, and M. Stutzmann, *Appl. Phys. Lett.* 69, 1749 (1996).
- [2.10] A. Yasan, R. McClintock, K. Mayes, S. R. Darvish, H. Zhang, P. Kung, M. Razeghi, S. K. Lee and J. Y. Han, *Appl. Phys. Lett.* 81, 2151 (2002).
- [2.11] T. Mori, T. Kozawa, T. Ohwaki, Y. Taga, S. Nagai, S. Yamasaki, S. Asama, N. Shibita, and M. Koite, *Appl. Phys. Lett.* 69, 3537 (1996).
- [2.12] H. Amano, N. Sawaki, I. Akasaki, and Y. Toyoda, *Jpn. J. Appl. Phys.*, Part 2 28,

L2112 (1989)

[2.13] X. Guo, and E. F. Schubert, Appl Phys. Lett. 78, 3337, (2001).

[2.14] X. Guo, and E. F. Schubert, J. Appl Phys. 90, 4191, (2001).

[2.15] H. Kim, S. J. Park, H. Hwang, N. M. Park, Appl Phys. Lett. 81, 1326, (2002).

[2.16] J. J. Wierer, D. A. Steigerwald, M. R. Krames, J. J. O'Shea, M. J. Ludowise, G. Christenson, Y.-C. Shen, C. Lowery, P. S. Martin, S. Subramanya, W. Götz, N. F. Gardner, R. S. Kern, and S. A. Stockman., Appl. Phys. Lett. 78, 3379 (2001).



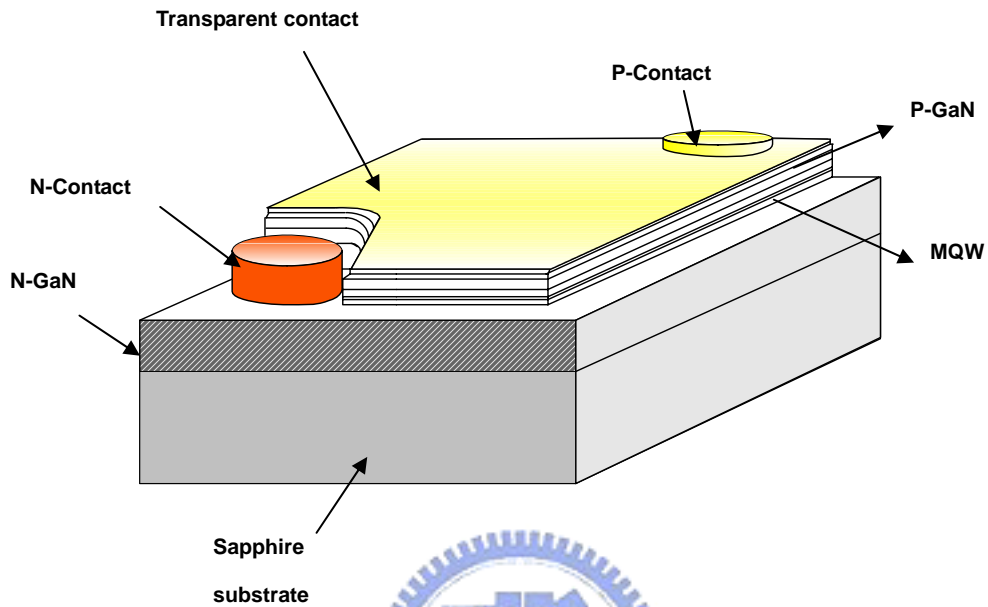


Figure2-1 The basic structure of GaN

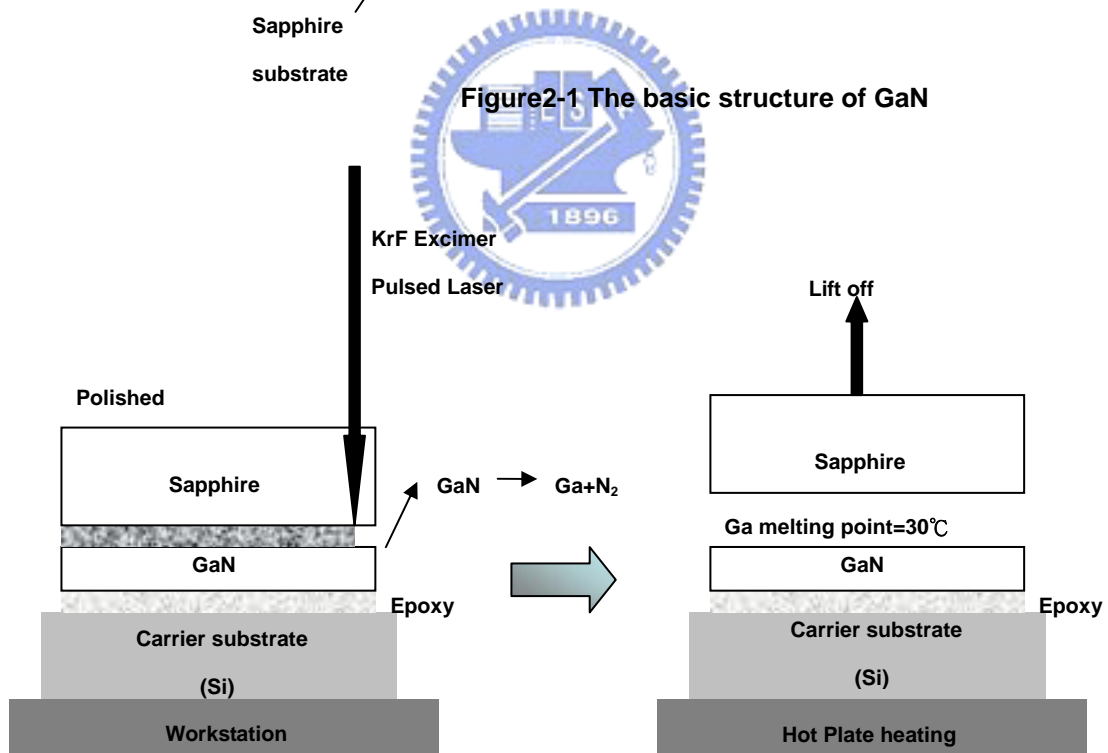


Figure2-2: The process scheme for fabrication of LLO un-doped GaN

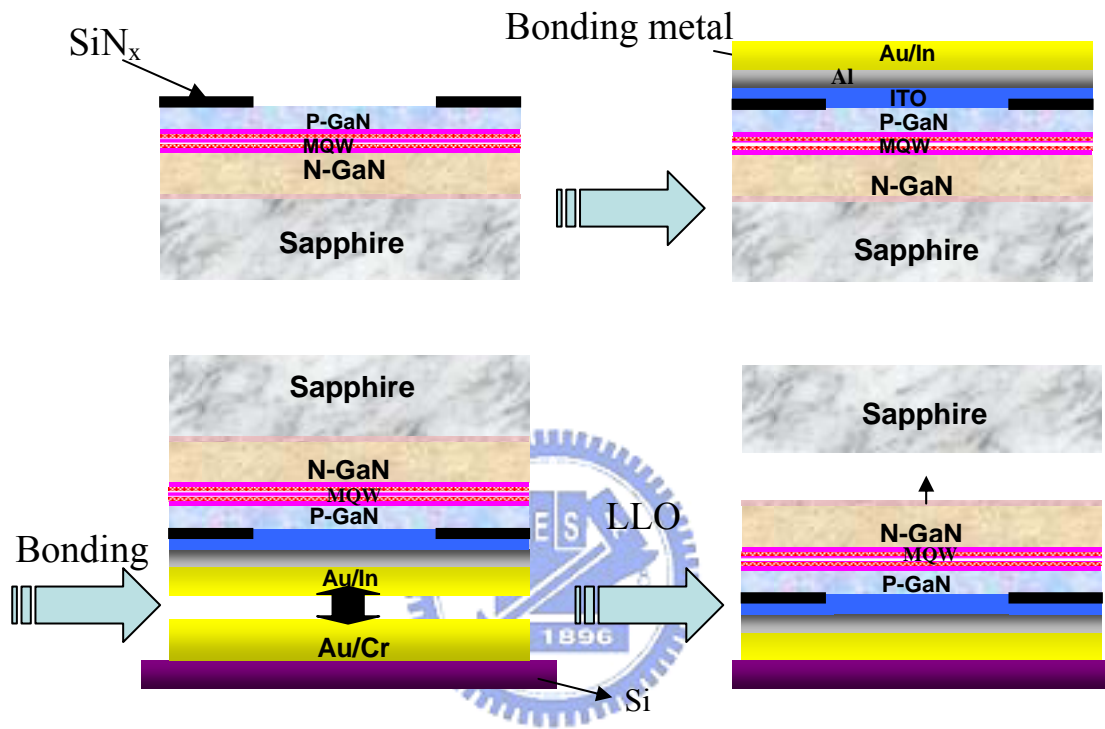


Figure 2-3 The processing of vertical light emitting diodes

Chapter 3

The progress of dry etching using by ICP-RIE

In this chapter, we report the progress of dry etching using by inductively coupled plasma reactive ion etching (ICP-RIE) for micro lens array and n-GaN surface roughening. The content consists of the introduction of photoresist, the re-flow of photoresist, the proportion of gases and the ICP bias for plasma etched. Finally, the images of etching result were taken by the scanning electron microscope (SEM).

3-1 Micro-lens formed by re-flow of photoresist

We use the well-known PR-reflow and dry-etching technique to fabricate n-GaN micro lens, and the basic method are well described in the literature.[3-1~3] The PR used in our experiments is AZ-5214E. An array of circular PR patterns with various diameter sizes is defined on an n-GaN film by the standard photolithography technique. The samples are then baked on hot plate, 168°C. The Si substrate transition temperature and PR start to flow. At the initial stage, the center was thinner and increased the circumference. As the temperature is further increased, the viscosity of the PR decreases, and the patterns eventually become convex with the center of each pattern the thickest. The smaller the diameter of the circular PR pattern, the lower the temperature required for convex shape formation. When the PR layer thickness and the baking temperature are 2.1 μ m and 168°C, pattern diameter below 20 μ m produce convex PR lens in a reproducible manner. Throughout the experiments the PR baking time is kept at 35min for consistency. Figure 3-1 shows the progress of micro lens formed by re-flow of photoresist.

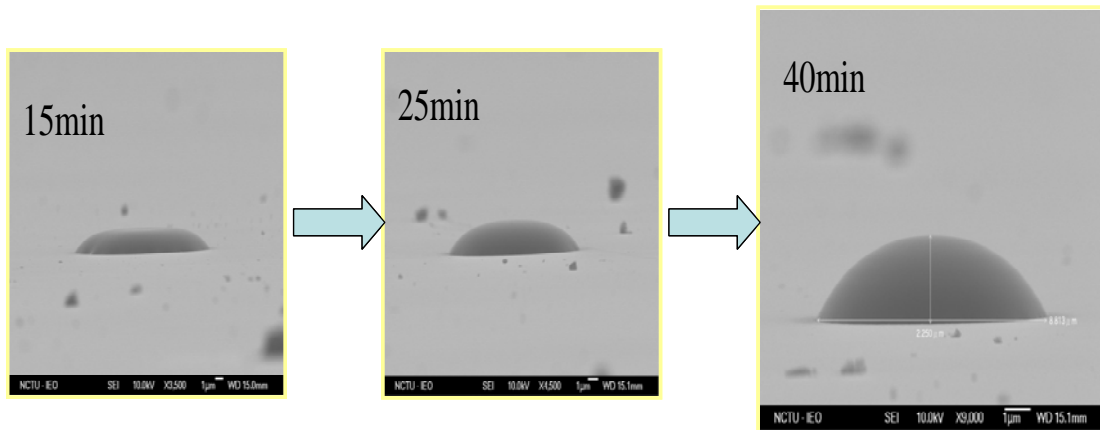


Figure 3-1 The progress of micro lens formed by re-flow of photoresist

3-2 The etching result of micro lens array by ICP-RIE

At first, the micro-lens array with various diameter sizes was defined on an n-GaN film on sapphire by the standard photolithography and photoresist reflow technique. Then, the sample was etched by using ICP-RIE. The parameters we used is $Cl_2/Ar= 40/5$ sccm, ICP power=550W, Bias=150W, 5mTorr. At this condition, the GaN etching rate was 330nm/min and the etching selectivity of GaN to photoresist was 0.58 for the n-GaN film that is on sapphire substrate. Figure 3-2 shows the SEM images of etching result, we can observe the planar and the micro lens, the planar is next to flat but the circumference of micro lens have the rod. In same condition, we also fabricated micro lens on laser lifted off n-GaN and etched by the same recipe as shown in Figure 3-3. It shows not only rods happened on the planar but also on the micro-lens. The planar also generated the rod and was not flat. The micro lens still had the rod. Therefore, we in order to improve the etching surface adjust the proportion of gas and the ICP bias for plasma etched.

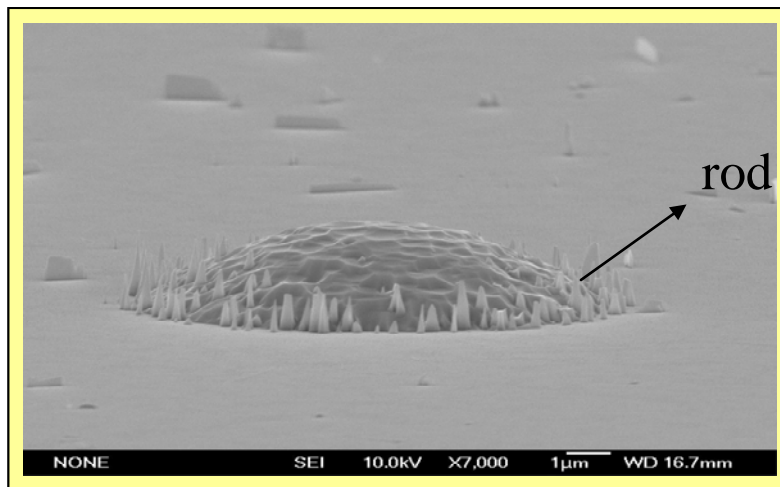


Figure 3-2 The SEM images of etching result, the micro lens is fabricated on the basic structure

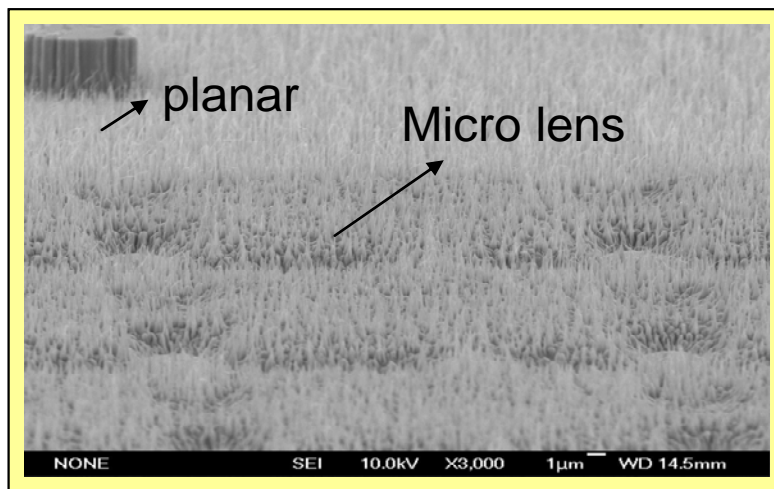


Figure 3-3 The SEM images of etching result, the micro lens is fabricated on vertical light emitting diode

The main parameters of dry etching we discussed here are the mixture of gases and bias power.

Mixture of gases

Several reports had indicated the use of BCl_3 is helpful to the improvement of

etching surface roughness for III-nitride compounds. In this section, we increased the ratio of BCl_3 and Cl_2 to understand the effect of the gases mixture on etching surface. Figure 3-4 shows the results under different ratio of BCl_3 and Cl_2 . With increasing the ratio, the surface roughness of micro-lens indeed becomes lower. However, the rod shape roughness always exists on the top of micro-lens in all these three conditions.

Bias power

In this experiment, we turned down the bias power to decrease the bombardment damage of photoresist. Figure 3-5 shows the etching results under different bias power conditions. Obviously, the bombardment damage of photoresist could be eliminated as the bias power is lower than 75W.

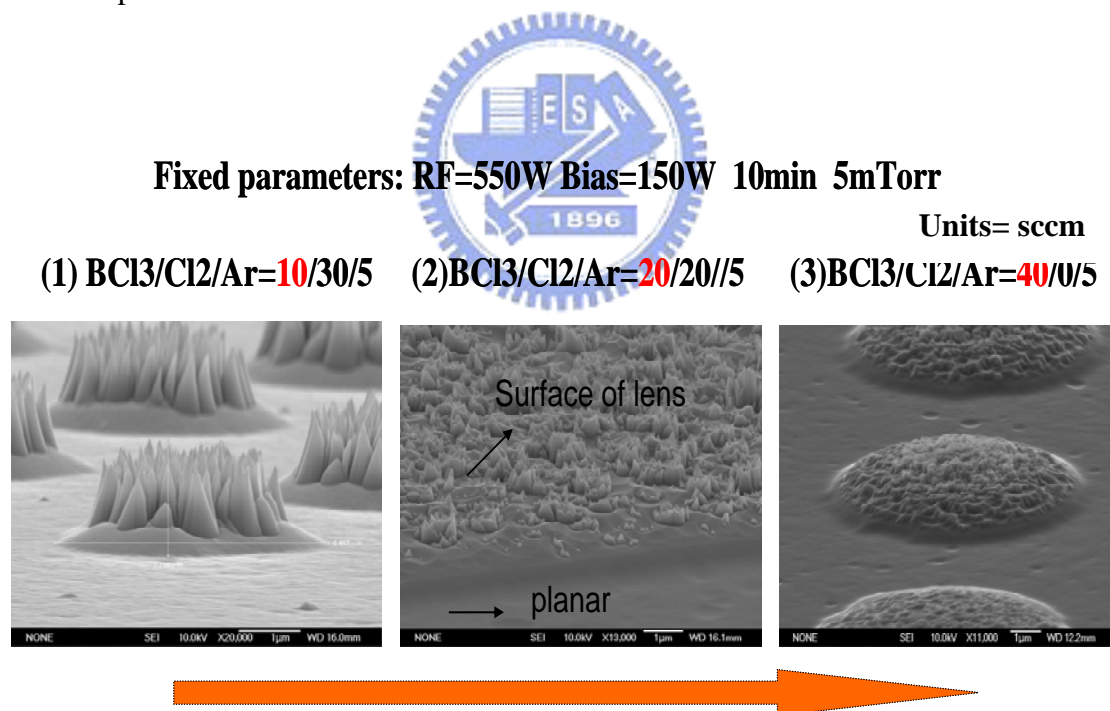
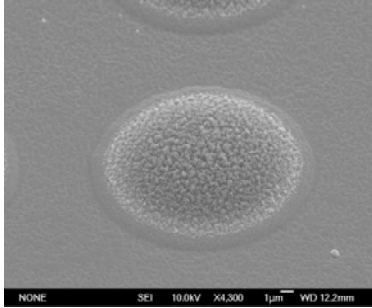


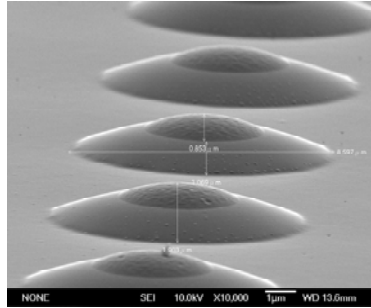
Figure 3-4 With increasing the ratio of BCl_3 , the SEM image of etching result

Fixed parameters: BCl₃/Ar=45/0 ICP=550W 5mTorr t=6min

(1) Bias=100W



(2) Bias=75W



(3) Bias=50W

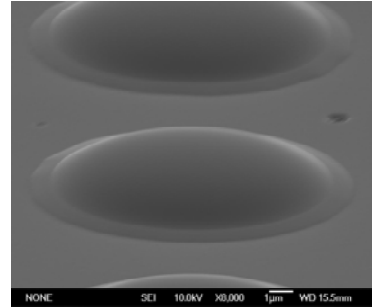


Figure 3-5 As the bias decreasing, the SEM images of etching result

Finally, the dry etching was performed in a gas mixture of BCl₃/Ar = 45 /0 sccm with an ICP source power of 550 W, a bias power of 50 W, etching time of 25min ,and a chamber pressure of 5 mTorr. At this condition, the GaN etching rate was 100nm/min and the etching selectivity of GaN to photoresist was 0.58. The etching was performed until the photoresist was etched away. Then, the GaN micro lens was formed on the LLO n-GaN surface. Figure 3-6 shows the final result of micro lens array on VLEDs. The AFM image was shown in Figure 3-7. The surface RMS is 1.1nm.

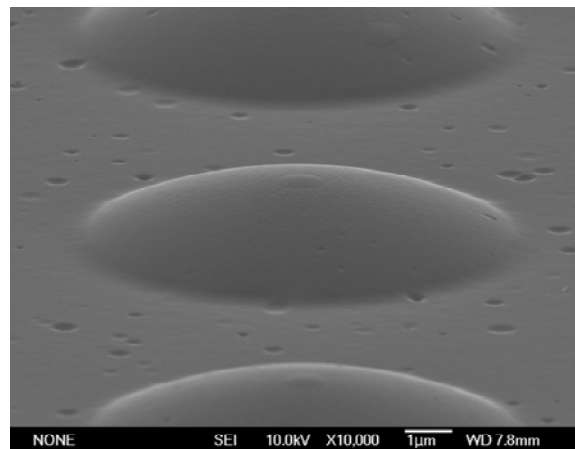
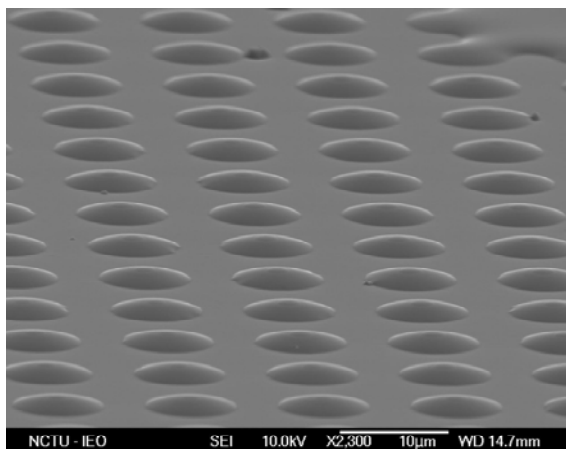


Figure 3-6The final result for micro lens array on vertical light emitting diodes

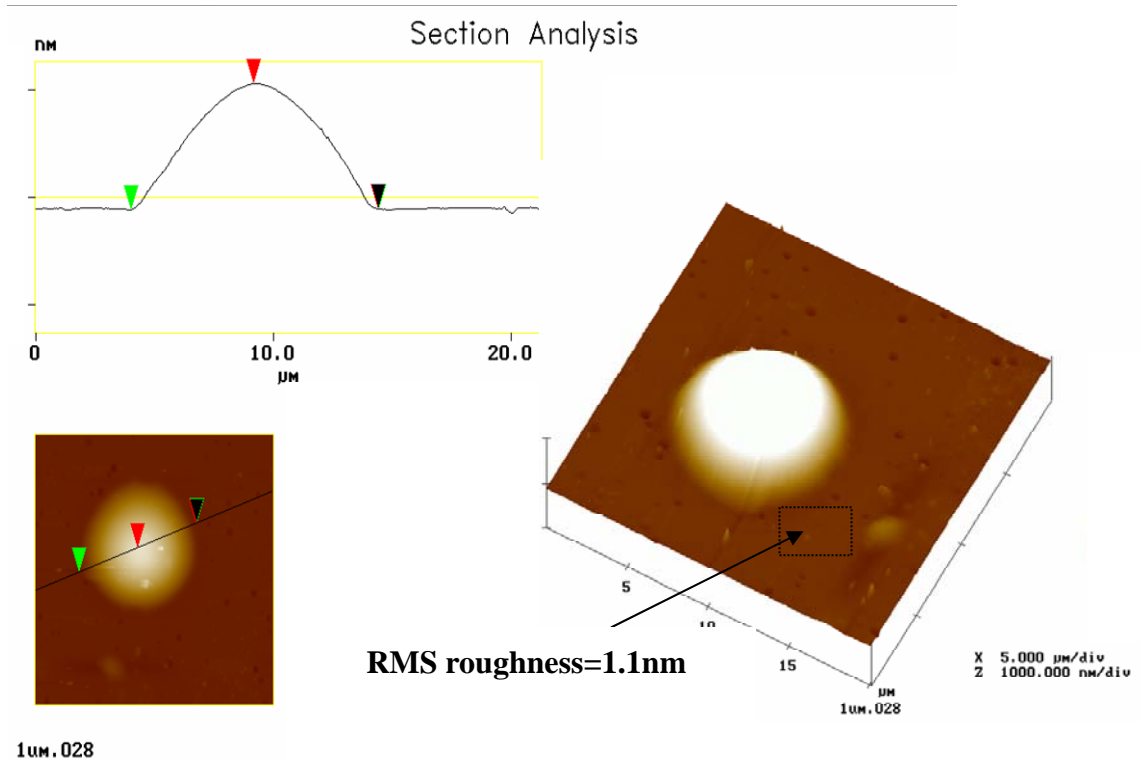


Figure 3-7 The AFM image of micro-lens



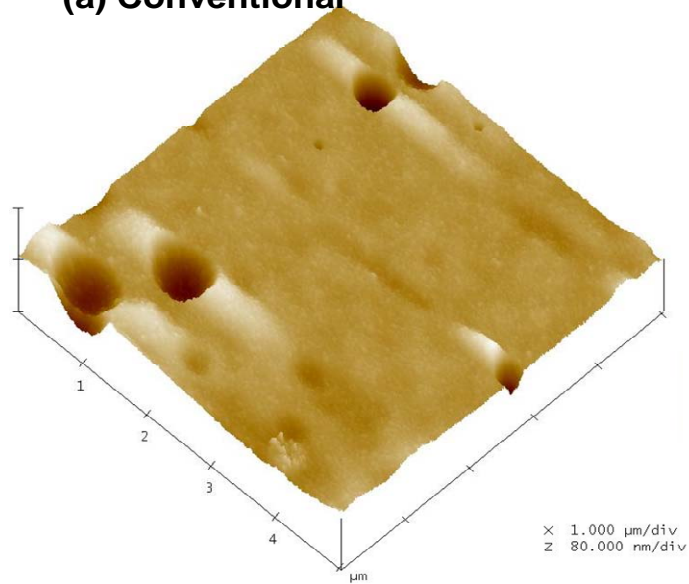
3-3 The progress of surface roughening for VLEDs

High power LED application is roughen the top surface of an LED is one of the methods for improving the light extraction. The roughening process was performed in an ICP-RIE. The parameters we used is $\text{Cl}_2/\text{Ar} = 30/5$ sccm, ICP power=550W, Bias=0W, 6mTorr. The n-GaN surface roughening was fabricated and the loss is not too much for n-GaN film. Figure 3-8 is an AFM image which shows the dry etching result at different etching time (conventional, 1min, 3.5min and 5min). The root mean square (RMS) roughness was obtained to be 1.2nm, 7.4nm, 32.9nm and 44.5 nm for conventional VLED, nano-roughened VLED with etching time of 1min, 3.5min and 5min, respectively. Obviously, the surface of VLED becomes more roughening as the etching time is longer. We could observe lots of granules were formed on sample

surface. In fact, the increase of roughness with the etching time increasing is because the size of the granules becomes larger. Using SEM, its size was found to be about 50nm, 150nm and 500nm at the etching time of 1min, 3.5min and 5min, respectively. Figure 3-9(a) shows the image of SEM for etching time=3.5min. Figure 3-9(b) is the image of SEM that compared surface before etching and after etching. In order to realize the cause of granules, we took the TEM photo as shown in Figure 3-10. In the figure, we could observe the dislocation exist in the bottom of those granules. This means the formation of granules could be partly attributed to the higher etching rate at the dislocation region generated than at other region. Of course, the relatively high etching rate of defects or those pits on LLO surface should be other possible reason to cause granules.



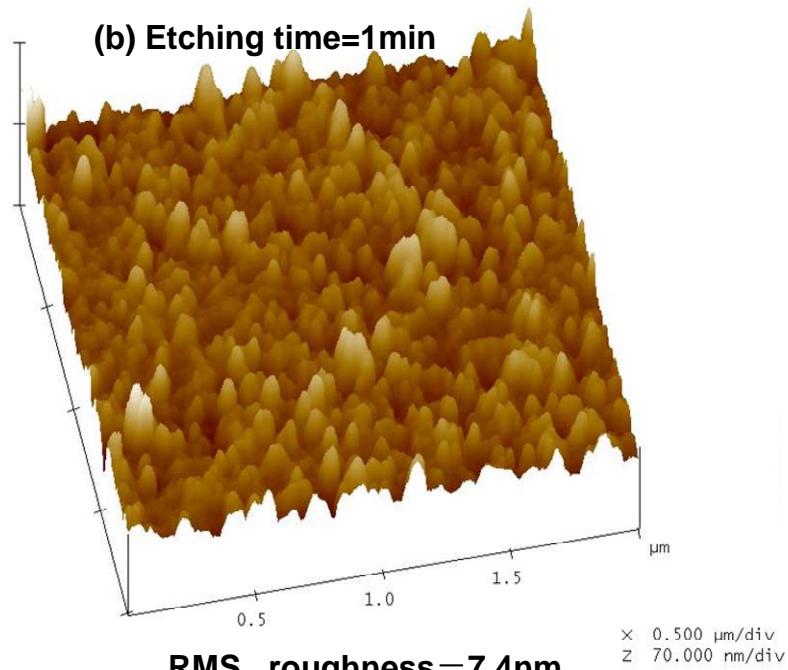
(a) Conventional



RMS roughness=1.2nm



(b) Etching time=1min



RMS roughness=7.4nm

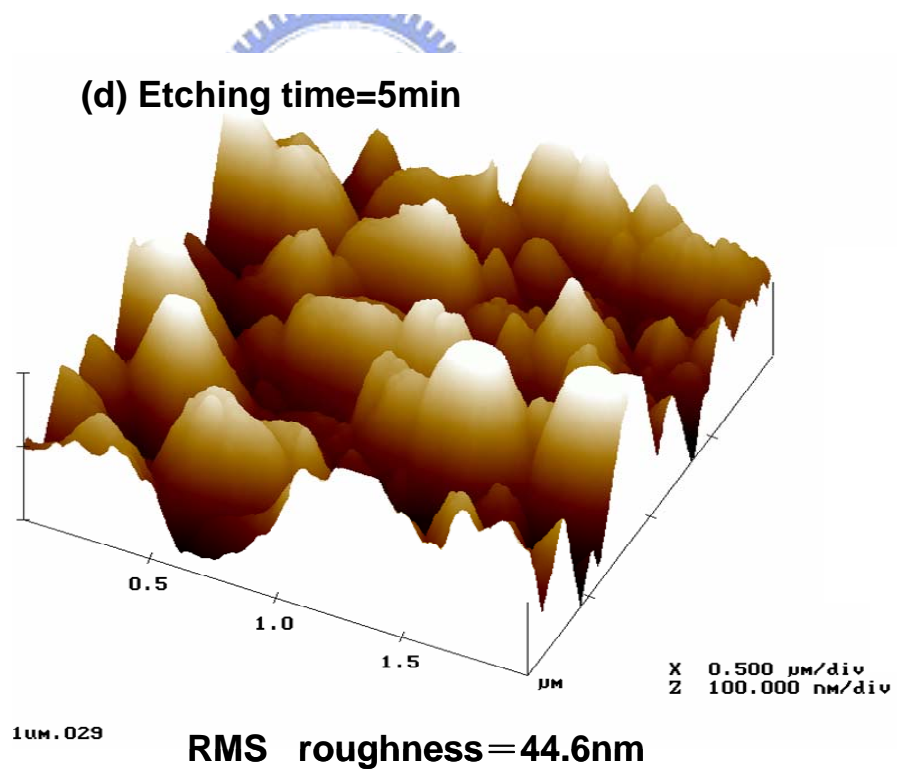
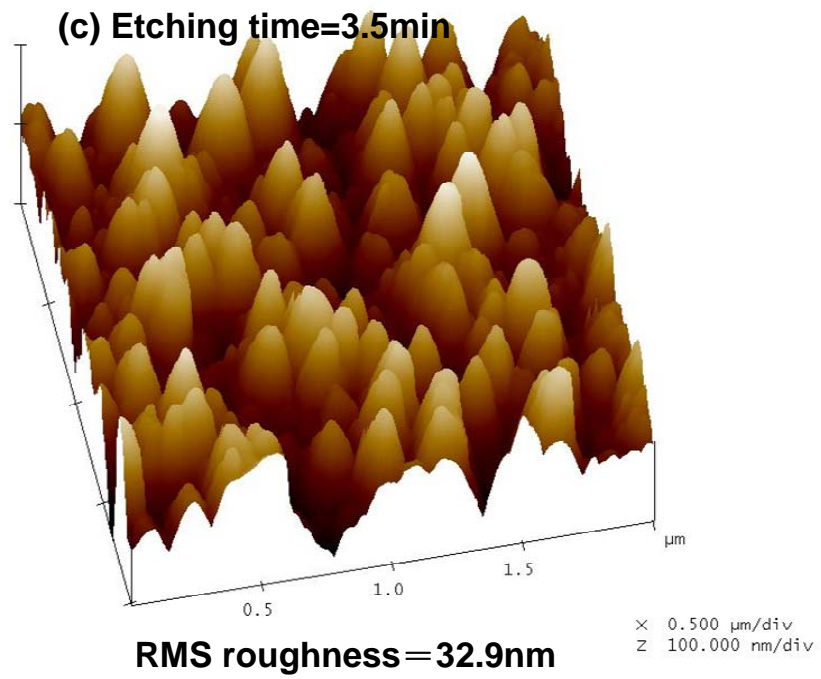
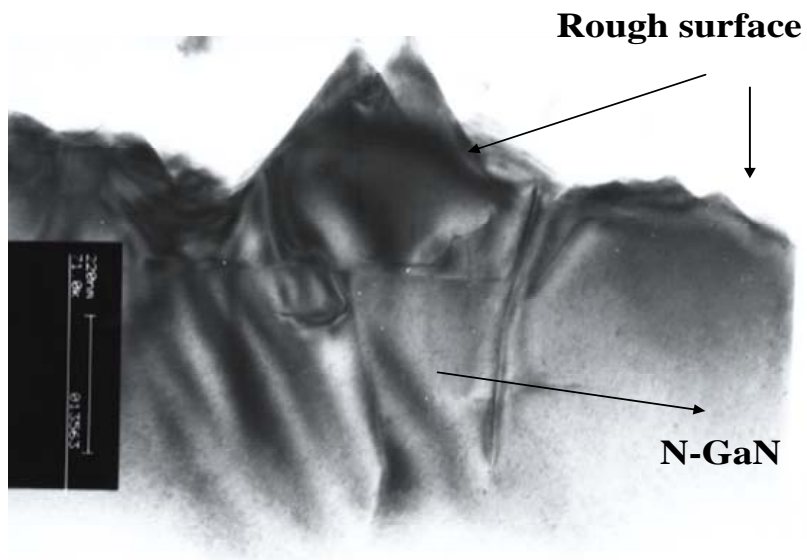
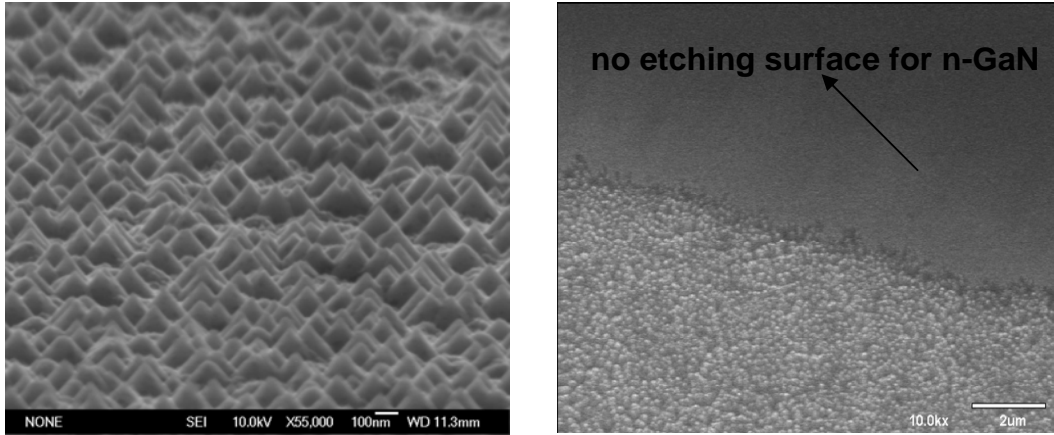


Figure 3-8 AFM image of an N-face GaN surface etched by ICP-RIE (a)conventional devices (b)1-min etching (c) 3.5-min etching and (d) 5-min etching



Chapter4

Fabrication and Characteristics of GaN VLEDs with Micro Lens Array

In this chapter, I demonstrate the fabrication and characteristics of GaN VLEDs with micro lens array. The size and coverage of micro lens on VLEDs, including of L-I-V, view angle were discussed. We compared our experiment data with the simulation results by Trace pro.

4-1 The Fabrication of GaN VLEDs with micro lens array

Figure 4.1 show the process of the GaN vertical light emitting diodes with micro-lens array. The process began with photolithography and photoresist reflow technique to form lens-shaped photoresist. AZ5214E photoresist was used and post baked. The detail of this process was discussed in 3-1. The photoresist lens was designed respectively, the photoresist lens was 3.5.10.15.20um and their height was 1.6-4.3um (see Table 4-1). Then, the dry etching was performed using on ICP-RIE with a gas mixture of $\text{BCl}_3/\text{Ar} = 45 / 0$ sccm, an ICP source power of 550 W, a bias power of 50 W, and a chamber pressure of 5 mTorr. At this condition, the etching rate of GaN was 100nm/min and the etching selectivity of GaN to photoresist was 0.58. The etching was performed until the photoresist was etched away and measured using a scanning electronic microscope (SEM) The height of GaN lens is shown in Table (4-1). Figure 4.2 shows the SEM image of GaN micro-lens with diameter of 10 μm

The sample was deposited a 2um SiO_2 film as etching mask and patterned by photolithography technique to define the mesa region of device and followed by the dry etching process. The mesa region of device is $300\mu\text{m} \times 300\mu\text{m}$. Finally, the trilayers of Ti/Pt/Au (20 nm/20 nm/100 nm) served as n-type ohmic contact that was deposited by an e-gum.

The electrical characteristics of VLEDs with micro-lens array and conventional VLEDs were both measured by probe station system and evaluated by injecting different current density. The device is driven by Keithley 238CW current source, and its light output from top view could be observed by CCD. Current-voltage (I-V) measurements were performed using the probe station and the data could be fee-backed to the computer from these facilities by a GPIB card. Figure 4.3 shows the electrical measurement system. The light output power was measured using a calibrated power meter with a large Si detector (detector area $10\times 10\text{ mm}^2$) approximate 5 mm above the device, collecting the light emitted in the forward direction.

4.2 Characteristics of GaN VLEDs with micro lens array

Figure 4.4 plots the current-voltage (*I-V*) characteristics of VLEDs with different size micro-lens (the space between micro-lens is kept to be 3 μm) and that of a conventional VLED fabricated on the same wafer. The forward voltage at 20mA (V_F) of conventional VLED and micro-lens VLEDs are almost the same (3.6V). The relation of light output power of our devices and driving current was plotted as shown in Figure 4.5. Figure 4.6 shows the emission image of VLEDs with 3 μm lens array at inject on current of 0.5mA and 1.0mA. Compared to the conventional VLED, micro-lens VLEDs all show a stronger light output power. We plotter the enhancement of light output power of VLED with different size micro-lens at 20mA of driving current as shown in the inset. Clearly, the enhancement varies from 18% to 30% as the size of micro-lens varies from 20 μm to 3 μm . Especially, the enhancement shows a relatively rapid increase as the size of micro-lens is smaller than 15 μm . This phenomenon seems to suggest our variation of enhancement with micro-lens size is related to the curvature radius of micro-lens. In order to simply realize this

phenomenon, we considered the micro-lens is next to the part of sphere in reality and used equation $r = (h^2 + a^2)/(2h)$ to calculate curvature of the different size lens, where 'r' is the curvature, 'h' is the height of micro lens and 'a' is the radius of micro lens. We could obtain the curvature = 1.96, 3.27, 7.48, 12.53 and 22.18 μ m for size of micro lens=3, 5, 10, 15 and 20 μ m micro-lens, respectively. In our structure of VLEDs, the n-GaN film is 1.85 μ m and MQW film is 0.05 μ m. It is noticeable that the curvature center of 3 μ m micro-lens is almost located at MQW considering the thickness of n-GaN and micro-lens. On the contrary, the curvature center of micro-lens rapidly far away MQW as the size of micro-lens is beyond 5 μ m, especially beyond 15 μ m. As shown in Figure 4-11, the light cone for photon escaping outside is the largest as the curvature center of micro-lens is located at MQW. This simply explains not only the largest enhancement of 3 μ m micro-lens but also the small enhancement variation as the micro-lens size is larger than 15 μ m. However, in order to clearly understand the actual effect of different micro-lens size on light output enhancement, we also need to consider the coverage of micro-lens. The coverage was defined as area of micro-lens/total emitting area. We kept the total area of micro-lens array to be $1620 \times 3^2 \times \pi$ (51% coverage) for VLEDs with different size micro-lens. The Figure 4.7 plots the L-I curve of conventional and micro-lens VLEDs and the enhancement of light output of micro-lens VLEDs. Similar to previous results, the light output power is also obviously enhanced as the size of micro-lens decreases. This again proves our explanation for the enhancement is reasonable. That is, the location of the curvature center of micro-lens determines the enhancement. However, compared with previous results, the enhancement of VLEDs with 5 μ m, 10 μ m, 15 μ m, 20 μ m lens was slightly lower. This should be due to less coverage of these size micro-lens compared with previous design. This also suggests the coverage of micro-lens array plays an important role for light extraction. The enhancement could be larger if we have

micro-lens array on VLEDs with larger coverage.

4.3 Simulation of GaN VLEDs with micro lens array

4-3.1 Simulation software – TracePro

TracePro is a comprehensive, versatile software tool for modeling the propagation of light in imaging and non-imaging opto-mechanical systems. TracePro is a Monte Carlo ray tracing program that accounts for flux or light power in your optical system, as well as the irradiance or the distribution of light. In Monte Carlo raytracing, scattering and diffraction are treated as random processes. Instead of propagating a distribution of light, discrete samples of the distribution, or rays, are propagated with BSDFs (Bidirectional Scattering Distribution Functions) used as probability distributions for determining ray directions. Monte Carlo ray tracing has several advantages over finite element methods. A list from includes

- Geometry can be procedural
- No tessellation is necessary
- It is not necessary to precompute a representation for the solution
- Geometry can be duplicated using instancing
- Any type of BRDF can be handled
- Specular reflections (on any shape) are easy
- Memory consumption is low
- The accuracy is controlled at the pixel/image level

To use TracePro, you set up a model of your optical system within the program including optical and non-optical surfaces, and trace rays through the model.

4-3.2 Simulation of VLEDs with Micro Lens Array by Tracepro

We set up our structure in TracePro software. The size of device we simulated is $300\mu\text{m}\times 300\mu\text{m}$. The structure contains a $1.85\mu\text{m}$ -thick n-GaN; an active layer of five-period InGaN (2 nm)/GaN (8 nm) QWs; a $0.25\mu\text{m}$ -thick p-GaN, and bonding metal located at bottom of structure with reflectivity of 80%. The micro lens array was set up following the real condition (Table 4-1) . An absorbing box was placed very close to the device for simulating the intensity distribution of our devices. In this study, the propagation and reflection of light in the devices were examined by applying the ray tracing method in TracePro [4.1], [4.2]. The parameters used in all simulations of this work are shown in Table 4-2 and the emission power densities in the active regions of all devices were set identical in the simulation.

Figure 4-8 shows intensity distribution of GaN VLEDs with micro lens array simulated from the Trace Pro program. From the Figure4-9 we could see that the light intensity of GaN VLEDs with micro-lens is stronger than that of conventional VLED, especially, the region of micro-lens. This explains micro-lens could effectively enhance the probability for photons escaping outside VLED structure.

Figure 4.10 (a) and (b) show our simulation results and experimental data for comparison under the condition of fixed spacing (3um) and fixed coverage of micro-lens array, respectively. In both conditions, the experimental data is similar to the simulation results. That is, the enhancement increases as the lens size decreases. It also was a strong evidence to say that the enhancement of light output of our devices surely come from the micro-lens. However, some enhancement shift about 10% could be found between simulation and experimental data. This inaccuracy must comes from not perfect process (such as of bottom mirror during LLO procedure) or inaccurate parameters of simulation.

In summary, highly efficient GaN VLEDs with micro lens array were fabricated. Their characteristics were measured and compared with those of conventional VLEDs fabricated from the same wafer. The forward voltages at 20mA of conventional and micro-lens VLEDs were all around $\sim 3.6\text{V}$. As the size of micro-lens is $3\mu\text{m}$ and the coverage is 51%, the light output of the micro-lens array VLEDs shows largest 30%. This result is also consistent with simulation.



Reference

- [4.1] D. Eisert, and V. Harle, International Conference on numerical simulation of semiconductor optoelectronic devices, (2002).
- [4.2] C. C. Kao, H. C. Kuo, H. W. Huang, J. T. Chu, Y. C. Peng, Y. L. Hsieh, C. Y. Luo, and S. C. Wang, C. C. Yu, C. F. Lin, IEEE Photonics Technology Lett. 17, 19 (2005).



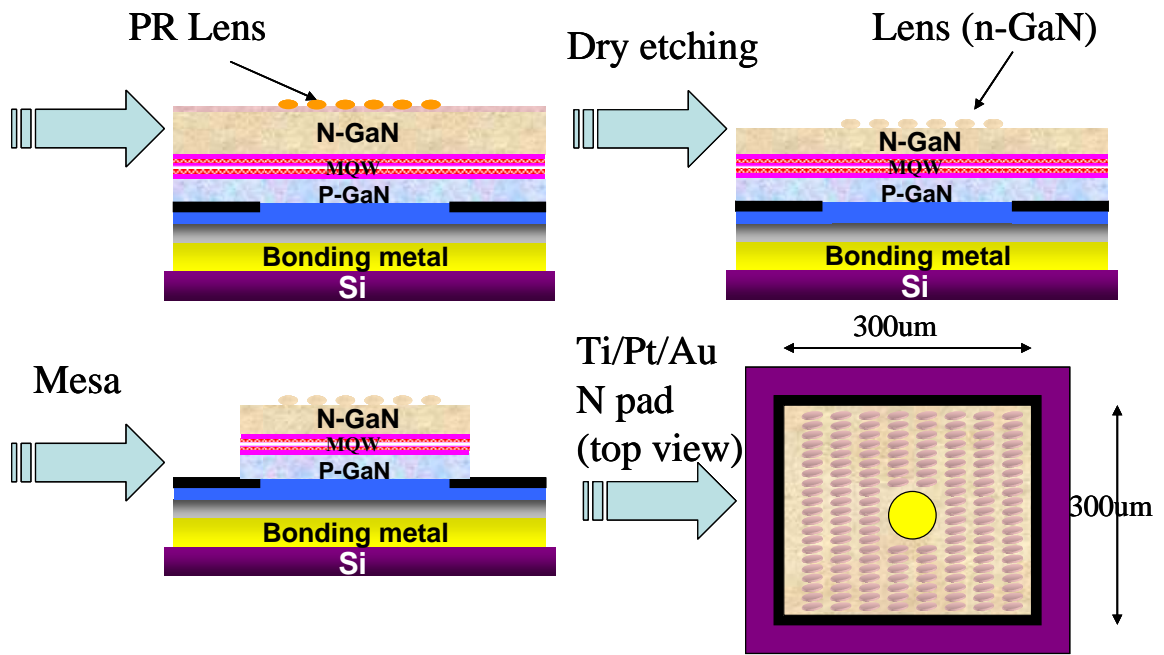


Figure 4.1 the processing of the GaN vertical light emitting diodes with micro-lens array

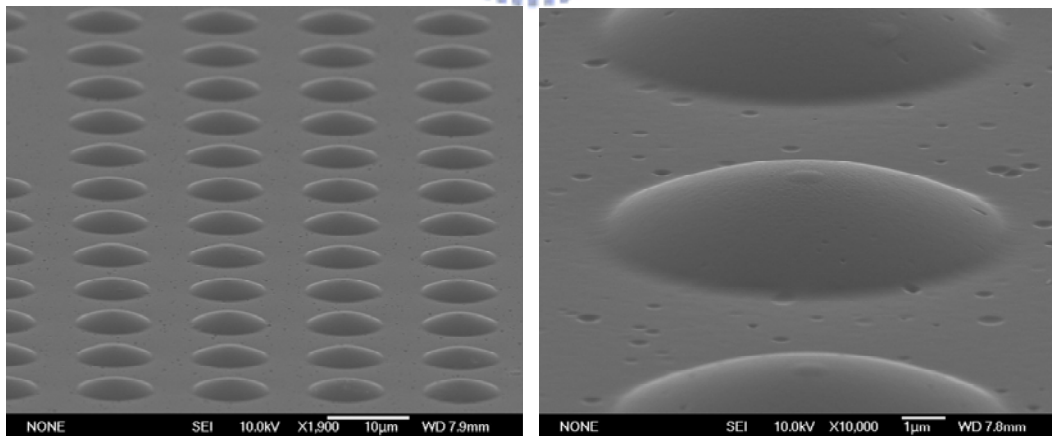


Figure 4.2 the SEM image of the GaN micro-lens array

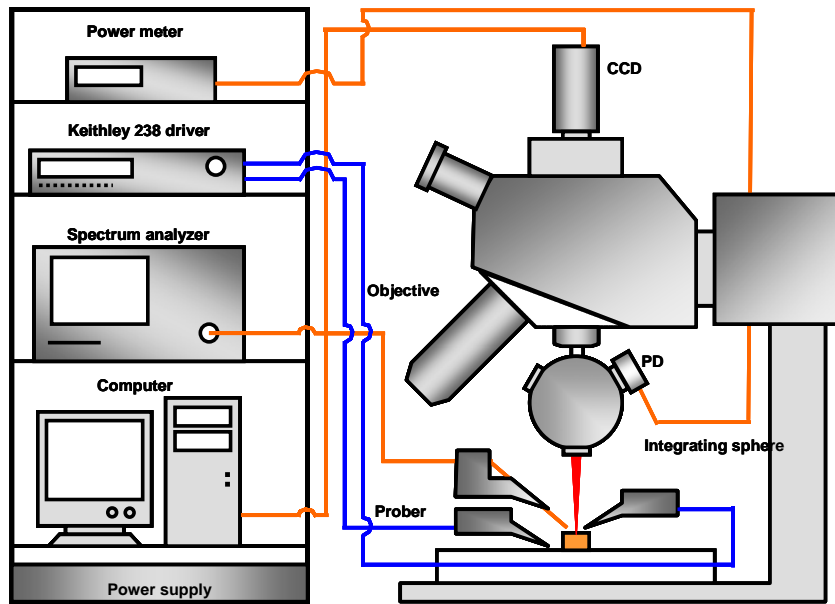


Figure4-3 The probe-station system is used for electronically characteristic measurements

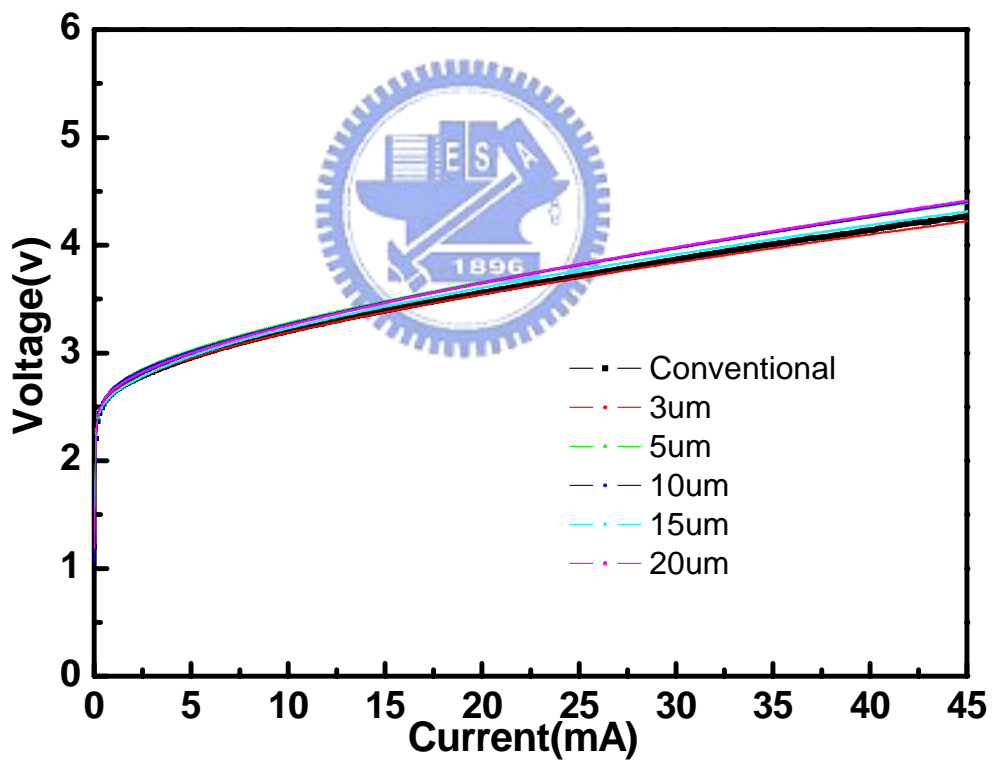


Figure4-4 Curves of current-voltage (I-V) of VLEDs with micro lens array and a conventional VLED fabricated from the same wafer.

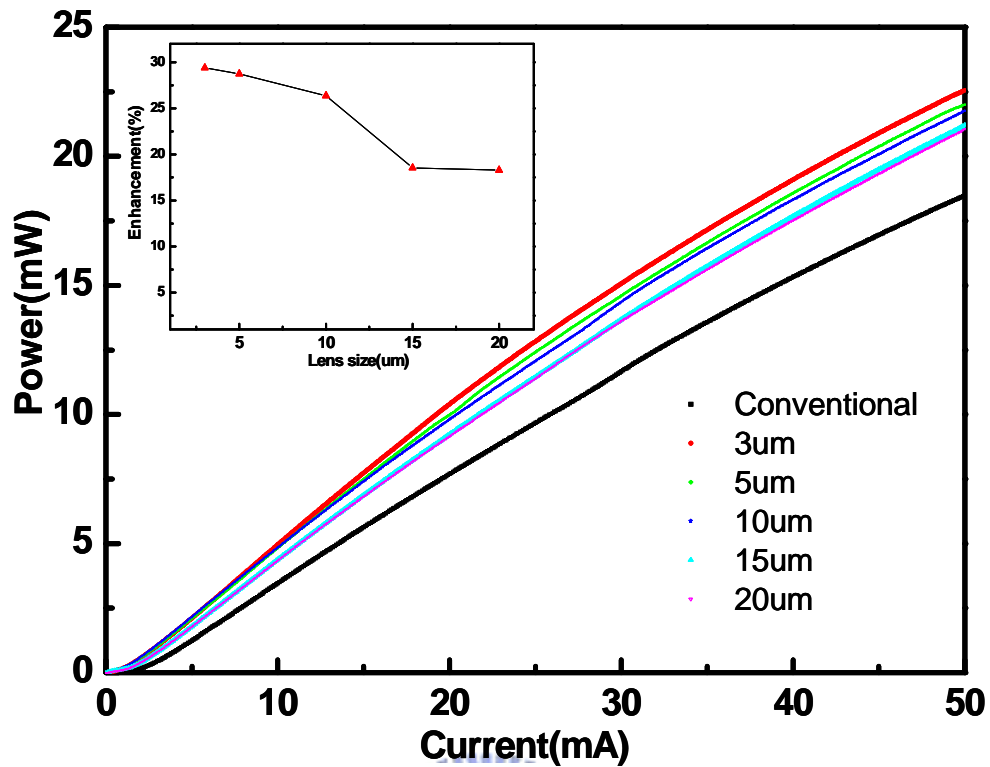


Figure4-5 Light output power of VLEDs with micro lens array and a conventional LED as functions of injected current density. The insert shows the enhancement-lens size curves.

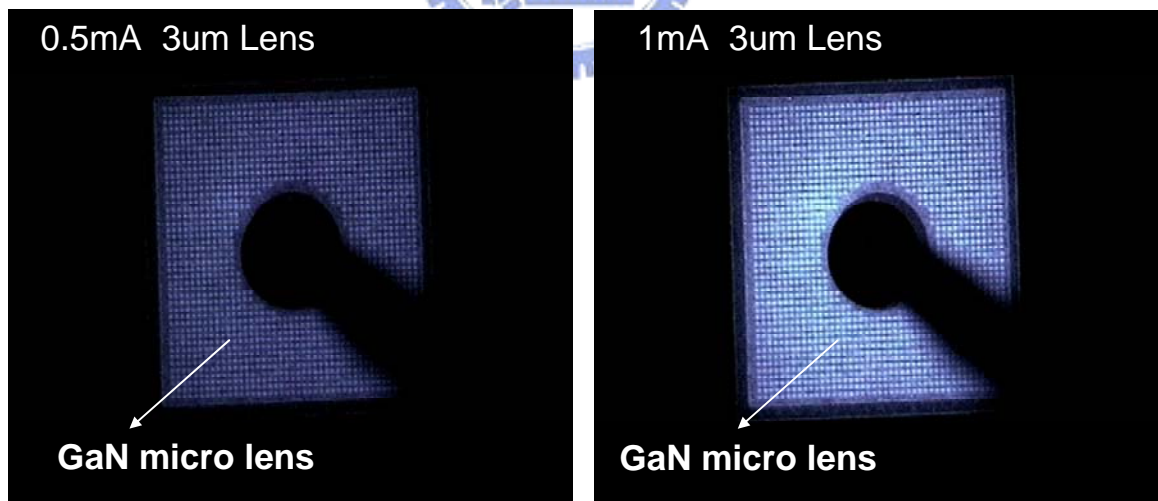


Figure4-6 the VLEDs with 3um lens array have injected 0.5 mA and 1.0 mA .

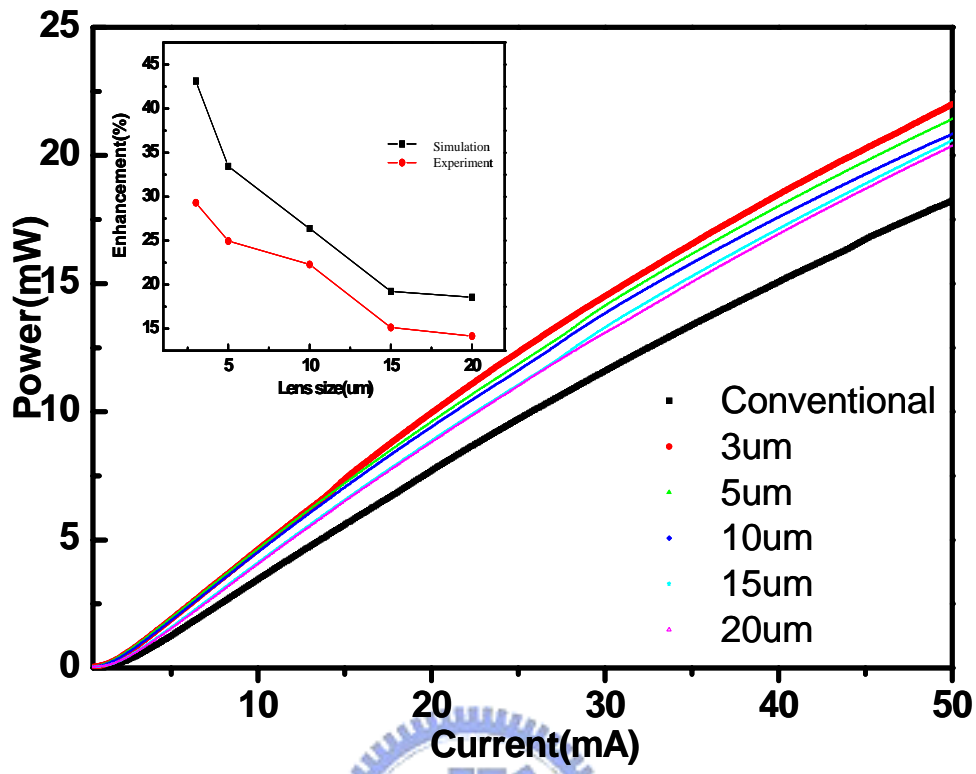


Figure 4-7 The same coverage for the different size lens. Light output power of VLEDs with micro lens array and a conventional LED as functions of injected current density. The insert shows the enhancement-lens size curves.

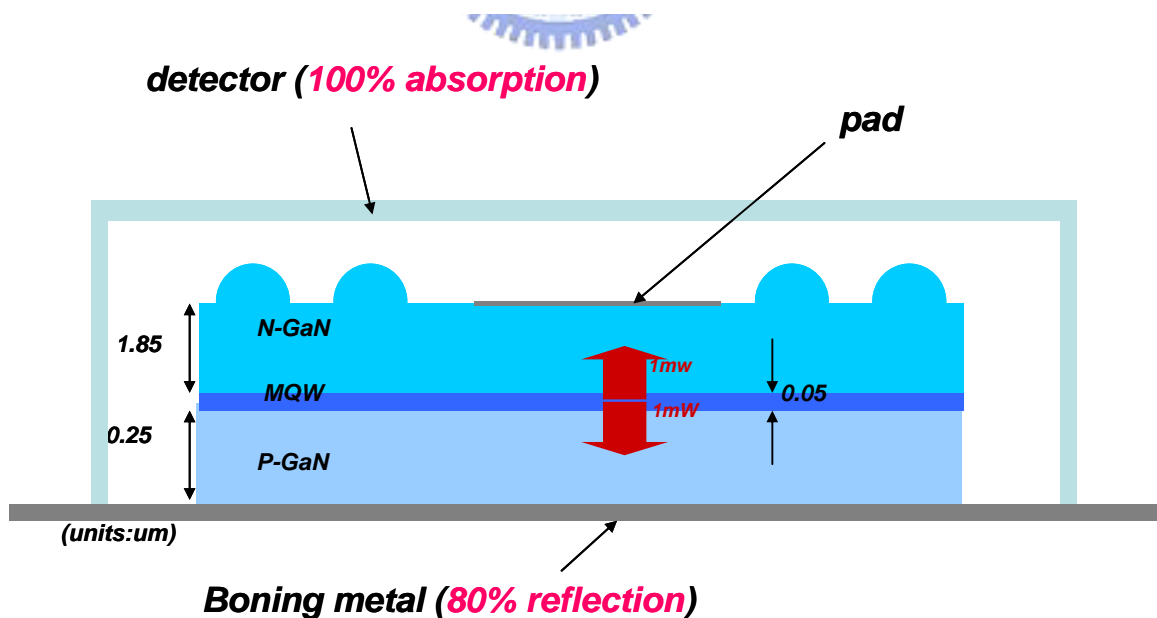
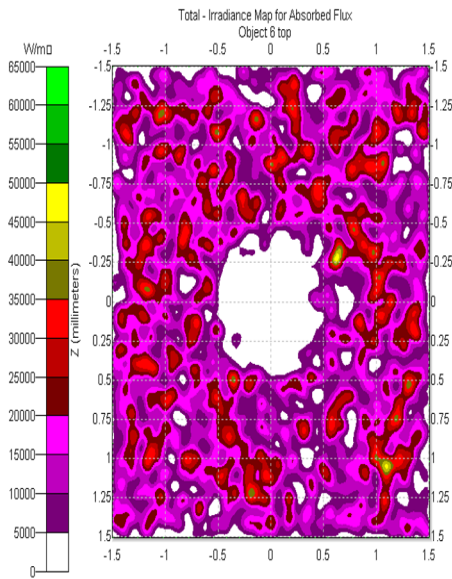


Figure 4-8 an irradiance map of GaN VLEDs with micro lens array of $300 \times 300 \mu\text{m}^2$ simulated from the Trace Pro program

Conventional



5um lens

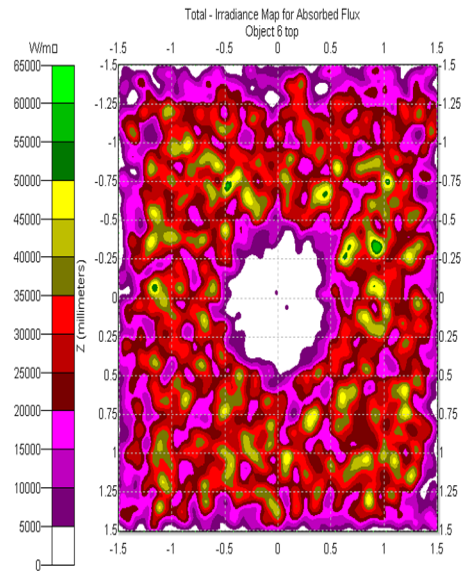


Figure 4-9 Light intensity distributed from the surface of detector box that is most next to the top surface of device by Trace Pro.

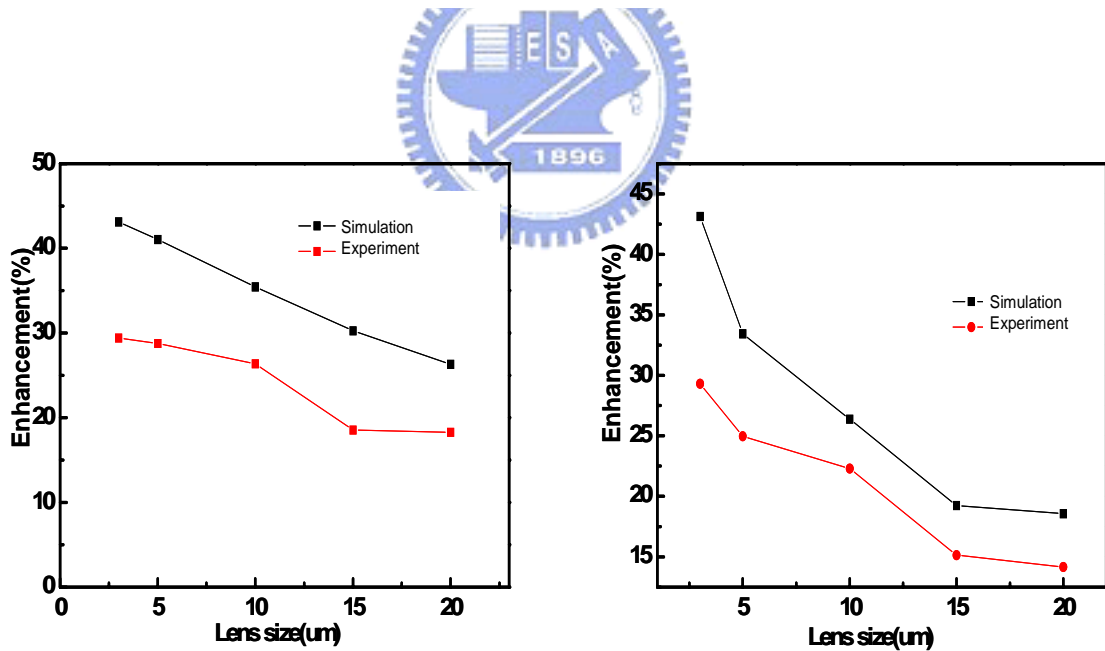


Figure4-10 (a) the experiment that fixed the space with different size of micro lens compared with simulation results. (b) the experiment that same coverage of micro lens compared with simulation results.

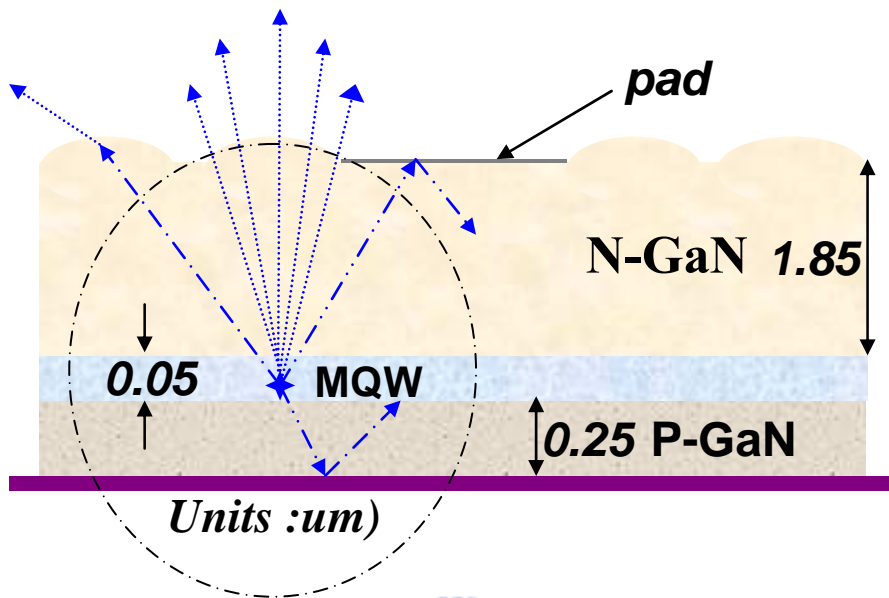


Figure 4-11 the light cone for photon escaping outsider is the largest as the curvature center of micro -lens is located at MQW

Hard bake (168°C) Time (45min)	Lens size	3um	5um	10um	15um	20um
Lens height (PR)/ Lens height (after etching) units (um)		1.61/0.71	1.99/1.16	3.36/1.92	3.81/2.12	4.30/2.38

Table 4-1 The height of different size of micro lens



Refractive index (n)		Reflection of Bonding metal (80%)	
n-GaN	2.5	Total power from	
p-GaN	2.5	the active region (mW)	2
Air	1	Absorption coefficient	100
MQW	2.5	($\lambda = 460 \text{ nm}, \text{cm}^{-1}$)	

Table 4-2 Parameters for the light-tracing simulation of VLED with micro lens array

Chapter5

Fabrication and characteristic of GaN VLEDs with surface roughening

In this chapter, I demonstrate the fabrication of GaN VLEDs with surface roughening, and we will discuss the scanning electron micrographs (SEM) image, the atomic force microscopy (AFM) image, the transmission electron microscopy (TEM) image of N-GaN surface roughening and performances of devices.

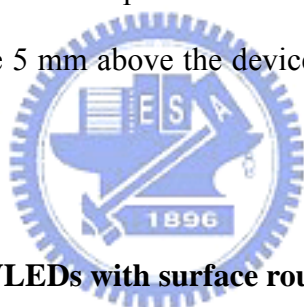
5-1 The Fabrication of GaN VLEDs with surface roughening

Figure 5-1 shows the process of the GaN vertical light emitting diodes with surface roughening which began 2-4 “the structure of vertical light emitting diodes”. At first, because of some treatments such as dry etching for roughening surfaces might cause electrical deterioration, we protected the surface of pad and passivation, the sample was deposited a 0.5 μm SiN_x thin film layer on GaN-based VLED film and followed by photolithography patterning. For n-GaN surface roughening formation, a dry etching method by inductively coupled plasma (ICP) self-aligned dry etching (Samco ICP-RIE). The dry etching was performed in a gas mixture of $\text{Cl}_2/\text{Ar} = 30/5$ sccm with an ICP source power of 500 W, a bias power of 0 W, and a chamber pressure of 6 mTorr. The roughness could be controlled by the etching time. In our experiment, we have three etching times: 1min, 3.5min and 5min for different devices. The result of etching described detailedly in chapter3.

Then, the sample was deposited a 2 μm SiO_2 film as etching mask and followed by photolithography patterning to define the mesa region of device, and dry etched the mesa of device (300 $\mu\text{m} \times 300\mu\text{m}$), Finally, the trilayers of Ti/Pt/Au (20 nm/20 nm/100 nm) for n-type ohmic contact were deposited by an e-gun. The diameter for circle n-type ohmic contact is 100 μm , the n-GaN film is 3.85 μm and MQW film is 0.05 μm

in our device. The conventional VLEDs with the same mesa size ($300\ \mu\text{m} \times 300\ \mu\text{m}$) were also fabricated from the same wafer for comparison. Figure 5-2(a) shows plan-view microphotographs of an VLED bonded on a Si substrate before roughening the surface and after roughening the surface is shown in Figure 5-2(b).

The electrical characteristics of VLEDs with surface roughening and conventional VLEDs were both measured by probe station system and evaluated by injecting different current density. The device is driven by Keithley 238CW current source, and its light output from top view could be observed by CCD. Current-voltage (I-V) measurements were performed using the probe station and the data could be fee-backed to the computer from these facilities by a GPIB card. The light output power was measured using a calibrated power meter with a large Si detector (detector area $10 \times 10\ \text{mm}^2$) approximate 5 mm above the device, collecting the light emitted in the forward direction.



5-2 Characteristics of GaN VLEDs with surface roughening

Figure 5-3 plots the current-voltage (*I-V*) characteristics with different etching times for the surface roughening LLO GaN VLED devices. All *I-V* curves showed linear characteristics up to 50mA. Because of the higher thermal conductivity of Si compared sapphire, these devices are advantageous for high-power operation. The forward voltage at 20mA, $V_F = 4.44, 4.43, 4.53$ and 4.55V for conventional VLED, nano-roughened with 1-min-etched, 3.5-min-etched and 5-min-etched, respectively. In this data, we could understand roughening surfaces might cause electrical deterioration in our case.

As shown in Figure 5-4, the output power from the surface of the chip versus dc injection current (*L-I*) characteristics for the VLEDs with different etching times. All *L-I* curves showed linear characteristics up to 50mA. The output power at a given

current increased with increasing etching time. As compared with the output power for a flat-surface VLED and the 10-min-etched surface VLED, the roughening treatment resulted in an increase of output power by a factor of 2.1 from the top surface. From other measurements on different etching time devices, the power also showed to enhance 30% and 95%. This output power measurement was performed from the upper side of the chip using a Si photodiode. It means that the power measurement is a relative output measurement from the top surface of the chip. Figure5-5 shows the VLEDs with surface roughening and conventional VLEDs at the same injected current 1mA, we could observe the relative intensity about output power.

In summary of the chapter, an etching method has been applied to a GaN-based VLED for the purpose of increasing extraction efficiency. VLED output test results have indicated that, presumably due to the decrease in light propagation in GaN film, there is a relationship between a roughened appearance and extraction efficiency. Although total integrated optical power has not been measured, the extraction efficiency from a top surface was increased 30% to 110% compared to that of a conventional VLED and the electrical properties of devices were similar. It is notable that the technique mentioned in this chapter is simple and does not require complicated processes, implying that it will be suitable for manufacturing of GaN-based VLEDs with surface roughening.

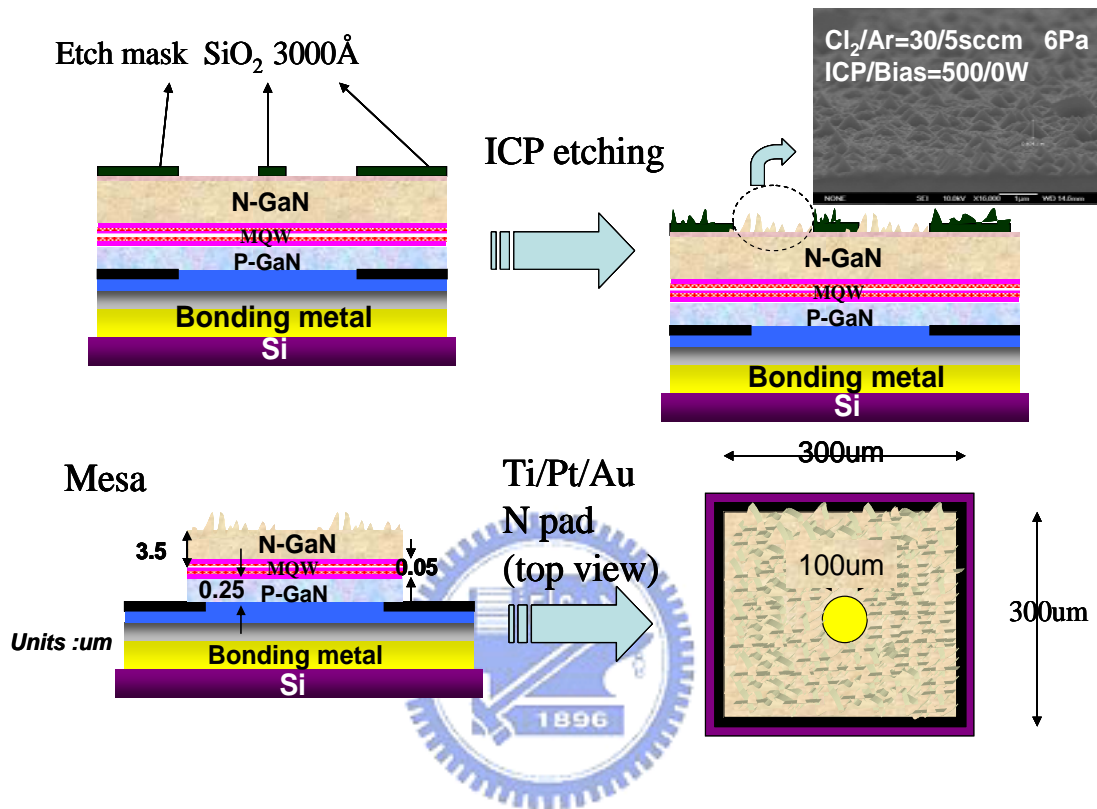


Figure 5-1 the processing of the GaN vertical light emitting diodes with surface roughening

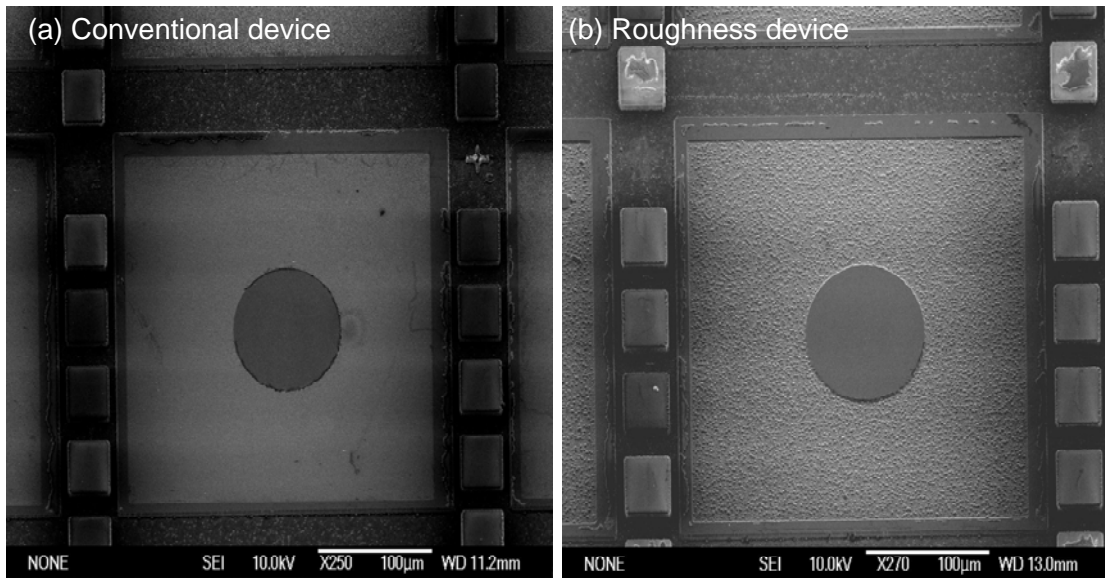


Figure 5-2 Plan-view microphotographs of a VLED bonded on a Si substrate: (a) conventional surface (b) after roughening the surface

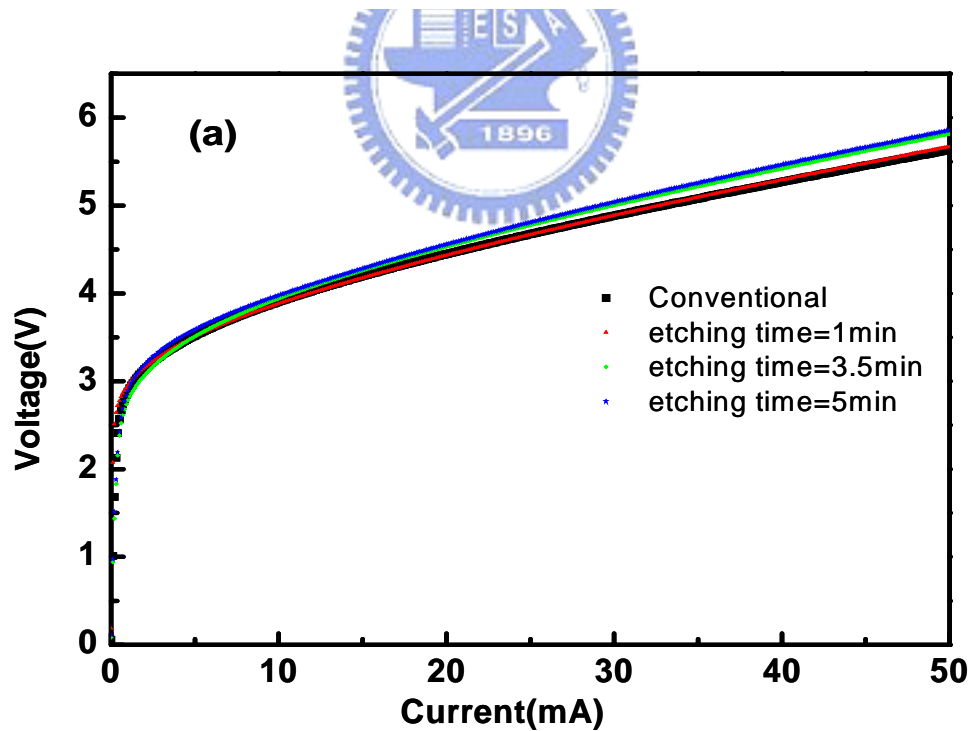


Figure5-3 Curves of current-voltage (I-V) of VLEDs with surface roughening and a conventional VLED fabricated from the same wafer.

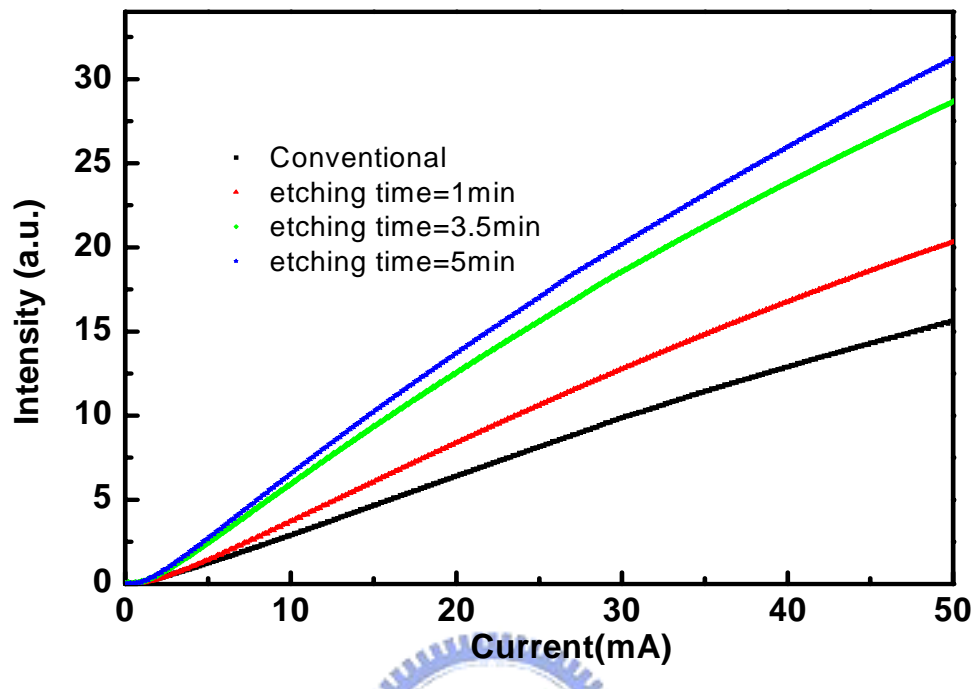


Figure 5-4 Light output power of VLEDs with surface roughening and a conventional LED as functions of injected current density

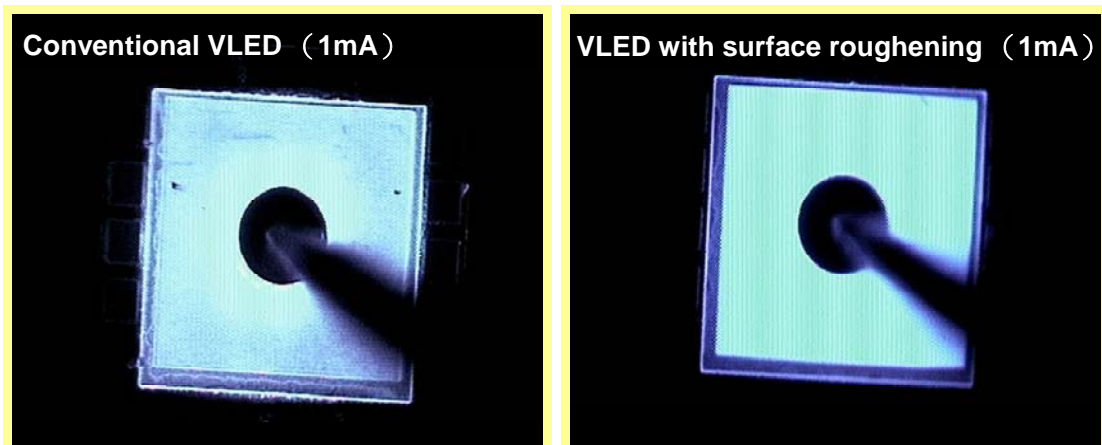


Figure 5-5 The VLEDs with surface roughening and conventional VLEDs at the same injected current 1mA

Chapter 6

Conclusion

In the thesis, we report the GaN vertical light emitting diodes with micro lens array and surface roughening. In first part, GaN-based VLEDs with micro lens array, photoresist micro lens diameter= 3、5、10、15 and 20 μ m, were fabricated with self-aligned technique, we use the well-known PR-reflow and dry-etching technique to fabricate n-GaN micro lens. The electrical and light output properties of VLEDs with micro lens array are studied and compared that of the conventional broad-area VLEDs. The forward bias voltage, V_F , of the GaN-based VLEDs at a driving current of 20 mA is similar as the conventional VLEDs \sim (3.6V). The light output from VLEDs with 3 μ m micro lens array was over 30% grater than that from conventional VLEDs with the same device areas. Besides, the enhancement factor of light output from the experimental data decreases as the size of micro lens increases and the area of micro lens array decreases. Then, we simulated by Trace Pro and the optimal designs for the GaN-based VLEDs with micro lens array are achieved in this work by the experiment and simulation methods.

In second part, we have fabricated successfully GaN based VLEDs with surface roughening. The n-GaN surface had roughened by plasma etching in order to increase the light extraction efficiency. The root mean square roughness of n-GaN surface increases as the etching time increases. The electrical and light output properties of VLEDs with surface roughening are studied and compared VLEDs without surface etched. The enhancement factor of light output from the experimental data also increases as the RMS roughness increases. Although total integrated optical power has not been measured, the extraction efficiency from a top surface was increased 30%~110% compared to that of a conventional VLED and the electrical properties of devices were similar. The forward voltages at 20mA of conventional and surface

roughened VLEDs were all around $\sim 4.5\text{V}$. It is notable that the technique mentioned in this thesis is simple and does not require complicated process, implying that it will be suitable for manufacturing of GaN-based VLEDs with surface roughening.

